Optimizing Sustainable Fertilizer Production: Techno-Economic and Environmental Assessment of Flexible Electrolytic Ammonia Production

Authors

Stefano Mingolla[1]*, Kevin Rouwenhorst[2,3,4], Paolo Gabrielli[5,6], Giovanni Sansavini[6], Magdalena M. Klemun[7,8]*, Zhongming Lu[1,7]*

↵* Corresponding authors. Email: smingolla@connect.ust.hk, zhongminglu@ust.hk, magdalena@ust.hk

Affiliations

[1]Division of Environment and Sustainability, The Hong Kong University of Science and Technology, Clear Water Bay, Kowloon, Hong Kong SAR, China
[2]Ammonia Energy Association, 77 Sands Street, Brooklyn, NY 11201, USA
[3]Catalytic Processes & Materials, MESA+ Institute for Nanotechnology, Department of Science & Technology, University of Twente, P.O. Box 217, 7500 Enschede, The Netherlands
[4]Koolen Industries, Europalaan 202, 7553 SC Hengelo, The Netherlands
[5]Department of Global Ecology, Carnegie Science, Stanford, CA 94305, USA
[6]Institute of Energy and Process Engineering, ETH Zurich, 8092, Zurich, Switzerland
[7]Energy Institute, The Hong Kong University of Science and Technology, Hong Kong SAR, China
[8]Division of Public Policy, Hong Kong University of Science and Technology, Clear Water Bay, Kowloon, Hong Kong SAR, China

Abstract

Ammonia production contributes about 1% of global carbon emissions due to fossil-based hydrogen production, and renewable-powered water electrolysis is a promising mitigation option. Yet, aligning the continuous Haber-Bosch (HB) process for ammonia production with variable renewable resources remains challenging. Increasing the HB process flexibility is a solution already adopted by the industry, but the conditions under which flexible plants can reduce costs remain unclear. Here, we address this issue by modeling and optimizing two plant configurations - continuous and flexible, both featuring on-site, semi-islanded, electrolytic hydrogen production with life-cycle carbon emission caps. Our results show that fully-flexible ammonia plants in wind-rich regions can be cost-competitive with current Steam Methane Reforming (SMR) derived ammonia while reducing life-cycle CO_2e emissions by over 90%. High flexibility minimizes grid import and storage costs, leading to lower Levelized Cost of Ammonia (LCOA) and decreased emissions. The renewable potential of a location, particularly the availability of abundant wind energy, is crucial for achieving a low LCOA and maximizing the emission reduction potential of flexible plants. Solar resources alone, however, cannot offset sub-optimal wind resources. In solar-dominated regions, plants with limited operational flexibility show a 7% increase in costs and emissions compared to continuous operation, primarily due to the higher reliance on battery storage and grid electricity import. Incorporating high flexibility in off-grid plants can halve costs, but semi-islanded facilities with grid connections remain more economical. Our findings offer valuable insights for plant operators, industry stakeholders, and policymakers, guiding effective strategies to decarbonize ammonia production.

Keywords

low-carbon hydrogen; electrolytic ammonia; flexible production; net-zero fertilizers; chemical industry decarbonization; energy system modeling

1. Introduction

Ammonia (NH_3) production is responsible for more than 1% of the world's carbon dioxide equivalent (CO_2e) emissions, with most of its carbon footprint being due to hydrogen production via Steam Methane Reforming (SMR) [1,2]. The volatility of natural gas prices and increasing concerns over climate change have sparked interest in alternative ammonia production methods [3]. Electrolytic ammonia, which uses renewable-powered water electrolysis to generate hydrogen and subsequently combines it with nitrogen for synthesis in the Haber-Bosch (HB) loop, is one such alternative to mitigate the industry's carbon emissions [4,5]. However, ammonia synthesis loops are typically designed and optimized for steady-state operation, close to their full capacity. As a result, these loops have limited flexibility and capability for accommodating reduced operation or fluctuating energy inputs [6]. One challenge lies in matching the operational requirements of the HB process with the intermittent nature of renewable energy.

To overcome this issue, one proposed solution is to locate ammonia plants in regions with high renewable energy potential and employ energy or hydrogen storage buffers to maximize annual operating hours. Recent studies by Nayak-Luke et al. [7] and Wang et al. [6] explored the effect of renewable energy intermittency on plant sizing and the Levelized Cost of Ammonia (LCOA) for off-grid plants, identifying the cost of renewable electricity as a key determining factor. Other studies also concluded that hybrid solar and wind energy systems are more cost-effective due to the complementary nature of solar and wind energy production patterns [8]. Yet, substantial energy or hydrogen storage buffers might be required to ensure continuous operation of the HB subsystems, potentially accounting for up to 40% of the plant costs [9].

Another potential solution is to connect the plant to the grid to ensure constant production. However, in this case, ammonia production becomes vulnerable to electricity price shocks, and relying solely on grid electricity could produce comparable, if not higher, emissions than fossil fuel-based ammonia, particularly in regions where electricity is carbon-intensive [10]. Furthermore, even if the grid is relatively clean, using it to produce electrolytic ammonia could strain regional resources, given an ammonia plant's large energy demands [11].

Recent research [12–14] has pointed to semi-islanded plants as a third, potentially advantageous solution. These plants, powered by renewable sources with backup grid connections, can significantly lower the costs of electrolytic ammonia/hydrogen production compared to off-grid plants. This approach, however, may involve operational emissions from imported grid electricity, particularly in carbon-intensive regions.

In response to the chemical industry's evolving landscape, characterized by a transition towards decentralized and flexible production [15], technology licensors are now focusing on transforming the rigid HB into a more adaptable and flexible one [7,16,17]. For example, licensors such as Topsoe [18] and Casale [9], claim that they can operate ammonia plants at 5-10% of their nominal load and rapidly ramp up or down as required. This would reduce the need for energy and hydrogen storage and leverage the variable output of renewable energies, potentially reducing over-capacities, lifecycle emissions, and costs. This level of performance is not a distant future concept but is already being put into practice. Topsoe, for instance, is playing a key role in two major projects aimed at taking advantage of this flexibility. The first is a collaboration with Skovgaard Invest and Vestas, which were awarded 11 billion euros to develop the first operational 'dynamic and green' ammonia plant in Denmark [19]. This plant is designed to be powered by renewable energy sources, specifically solar panels, and wind turbines, and is expected to set a precedent for future generations of ammonia plants. The second project is based in Inner Mongolia, where Topsoe is working to develop a flexible plant in Baotou, designed to run on onshore wind power [20].

Despite the recent trend in industry efforts, only a limited set of studies have examined flexible ammonia production. These studies have concluded that plant flexibility is key to reducing storage size and overall costs [6]. However, several technological advancements are still necessary to achieve a high level of flexibility, especially in the Air Separator Unit (ASU) and ammonia synloop, which are currently the least flexible plant systems [6,7,21].

Existing studies on electrolytic ammonia production have provided valuable insights, but they face recurring limitations that hinder a comprehensive understanding of this field and the derivation of general conclusions and recommendations.

Firstly, many of these studies are location-specific and their results may not be generalized to describe feasible and *optima* solutions in different geographical areas. Exploring scenarios where plants are not located in areas with high renewable potential is also crucial. We expand current analyses by considering diverse geographic and climatic conditions, hence providing a much-needed perspective for governments and industries planning to implement these technologies in different regions.

Secondly, previous research has often considered inflexible plants' subsystem components and used battery or hydrogen storage to handle intermittent renewable resources. While this approach reflects the current state of the industry, it does not account for recent advancements and future expected improvements. The industry has yet to see large-scale projects of electrolytic plants powered entirely by renewables. However, recent industry interviews suggest that future projects specifically designed for electrolytic plants could accommodate faster dynamics [22]. Failing to consider these trends could limit the applicability of the research findings. There is a gap in the literature when comparing electrolytic plants with continuous 24/7 ammonia output (a common practice today) to highly flexible plants that eliminate the need for energy or hydrogen storage. Storing hydrogen in high-pressure tanks is costly and presents safety concerns. Comparing these two plant configurations is critical to understanding the benefits and challenges associated with each design, enabling decision-makers to choose the most suitable option based on their circumstances.

Lastly, despite the urgent need to reduce carbon emissions, only a few studies have considered deep decarbonization scenarios for ammonia production. Policymakers aiming to decarbonize the industry need information about how much emissions can be reduced in different regions, under different scenarios, and different assumptions regarding subsystems performance and plant configuration. Only a handful of studies, such as Campion et al. [13], have considered the implications of carbon emissions in their analysis. However, their analysis primarily covers emissions resulting from grid usage. A more holistic approach to carbon emissions, including potential sources from all stages of the production process, is needed to fully understand the environmental implications of electrolytic ammonia production.

In response to these limitations, we develop a modeling framework and optimization approach for large-scale, semi-islanded electrolytic ammonia plants under different renewable energy profiles. These profiles are based on representative regions across Europe, each with unique weather patterns and renewable energy potential. The focus on the European continent is motivated by the European Union's strong interest in decarbonizing its industry through electrolytic production [23], especially considering the significant damages caused by the 2022 energy crisis, which exposed the industry's vulnerability to price shocks [24,25]. The selected representative regions include those with high-capacity factors for both solar and wind energy, regions with moderate renewable conditions, and regions with poor renewable potential. We also consider regions dominated by solar or wind energy to ensure a comprehensive analysis. We compare various plant layouts, including continuous and flexible configurations, while considering different degrees of flexibility. The optimization is based on Mixed-Integer Linear Programming (MILP) and determines the minimum-cost design and operations of ammonia production plants. Additionally, we conduct a comprehensive sensitivity analysis to evaluate the impact of key parameters on the system's performance, cost, and lifecycle emission.

The primary goal of this work is to determine whether increasing plant flexibility can reduce the costs of electrolytic ammonia production, making it cost-competitive with fossil-based standards. In particular, the study aims to understand the impact of renewable energy potential on the optimal design, operation, and configuration of ammonia plants, as well as the resulting LCOA and carbon content. Additionally, the research investigates how the flexibility of key subsystems influences the economic feasibility and lifecycle carbon emissions of both flexible and continuous ammonia production. By identifying and analyzing the critical input parameters that affect the LCOA, this work assesses the sensitivity of the LCOA to changes in these parameters.

Our results show that location, with its associated renewable energy potential, is a more critical factor than plant configuration in influencing the economic viability and environmental impact of large-scale electrolytic ammonia production. Wind-rich areas outperform others economically, offering ammonia production costs comparable to traditional SMRs. These regions also benefit from a lower LCOA than areas with less wind. Plants with high flexibility configurations can reduce costs and emissions, especially in wind-dominant areas, while plants with partial flexibility operations may increase costs and emissions in solar-dominated regions.

Our research provides a critical foundation for industry decision-making regarding investment in research and technological development in the ammonia industry. Equally, it offers policymakers guidance on where to prioritize subsidies and support, potentially accelerating the transition to sustainable ammonia production. The unique insights revealed by our analysis thus serve as a vital tool for both industry stakeholders and policymakers in strategizing the decarbonization of ammonia production and aligning economic incentives with environmental objectives.

Nomenclature

Indices

t	index for time-steps (hours), $t \in \{0, 1, ..., T\}$ with $T = 8760$
l	index for years, $L \in \{0, 1, ..., L\}$ with $L = 25$

Sets

$\mathcal{J}$	set of energy carriers
$\mathcal{K}$	set of technologies
$\mathcal{K}_R$	set of renewable power technologies

Energy carriers

E	electricity
H_2	hydrogen
N_2	nitrogen
NH_3	ammonia

Technologies

PV	photovoltaic
WT	wind turbine
EL	electrolyzer
A	air separator unit
S	ammonia synloop
CP	hydrogen compressor
ST	hydrogen high-pressure storage tank
CT	ammonia cryogenic storage tank
B	battery energy storage system

Parameters

ω	capacity factor
D	plant output
p	energy price
γ	energy grids and technology carbon footprint
c	technology investment cost
v	technology operation & maintenance cost
η	technology performance
δ	technology minimum load
ρ	stoichiometric ratio hydrogen/ammonia by mass

Variables

U	input energy
V	output energy
M	imported electricity
N	exported electricity
P	technology installed capacity
b	technology selection
y	ON/OFF scheduling

2. Materials and Methods

In energy system modeling, MILP has emerged as the predominant optimization approach for the design and operation of multi-energy systems. MILP stands out due to its ability to effectively solve systems of linear equations, while including nonlinearities thanks to the introduction of binary variables, thus ensuring a trade-off between computational efficiency and solution robustness [12,26–28]. We formulate a MILP in Python with the Gurobipy package [29] and solve it with the commercial solver Gurobi [30].

We model and optimize two distinct ammonia plant setups, namely (i) a continuous plant and (ii) a flexible plant, as shown in **Fig. 1**. The objective function is to minimize the lifetime system cost (*eq. 1*), while the decision variables are the design and operation of the ammonia plants under different input parameter assumptions.

$$\min z_{cost} = \sum_{k\in K} I_k^{NPV} + \sum_{l=1}^{L}\sum_{k\in K} v_k^{NPV} I_k + \sum_{l=1}^{L} \frac{\sum_{t=0}^{T} (p_E M_{E,t} - p_{E,N} N_{E,t})}{(1+r)^l} \qquad \textit{eq. 1}$$

where z_{cost} represents the total lifetime cost of the electrolytic ammonia plant, consisting of the sum of capital cost $\sum_{k\in K} I_k^{NPV}$ operation and maintenance cost (O&M) $\sum_{k\in K} v_k^{NPV} I_k$, and grid power purchase and sell $\sum_{l=1}^{L} \frac{\sum_{t=0}^{T} (p_E M_{E,t} - p_{E,N} N_{E,t})}{(1+r)^l}$; In detail, L is the lifetime of the plant in years, T is the number of hours per year, I_k is the installation cost of technology k; v_k is a fraction of the installation cost for annual maintenance, p_E is the price of grid electricity for industrial end-users, while $p_{E,N}$ is the price at which electricity is sold back to the grid., $M_{E,t}$ is the quantity of imported electricity from the grid, and $N_{E,t}$ is the quantity of electricity exported. Further details regarding cost calculation are reported in SI - *eq. i-iii*.

$$LCOA = \frac{z_{cost}}{\sum_{l=1}^{L}\sum_{t=1}^{T} D_{NH3,t}^{h}} \qquad \textit{eq. 2}$$

The LCOA is computed through *eq. 2*. The LCOA represents the average cost per unit of ammonia produced, considering the time value of money and the expected operational lifetime of the production facility. We assume that the total amount of ammonia produced $\sum_{l=1}^{L}\sum_{t=1}^{T} D_{NH3,t}^{h}$ ($D_{NH3,t}^{h}$ is the hourly output of the plant), remains consistent regardless of the chosen plant layout or assumptions regarding input parameters. This allows for a meaningful comparison of LCOA across diverse scenarios and plant setups.

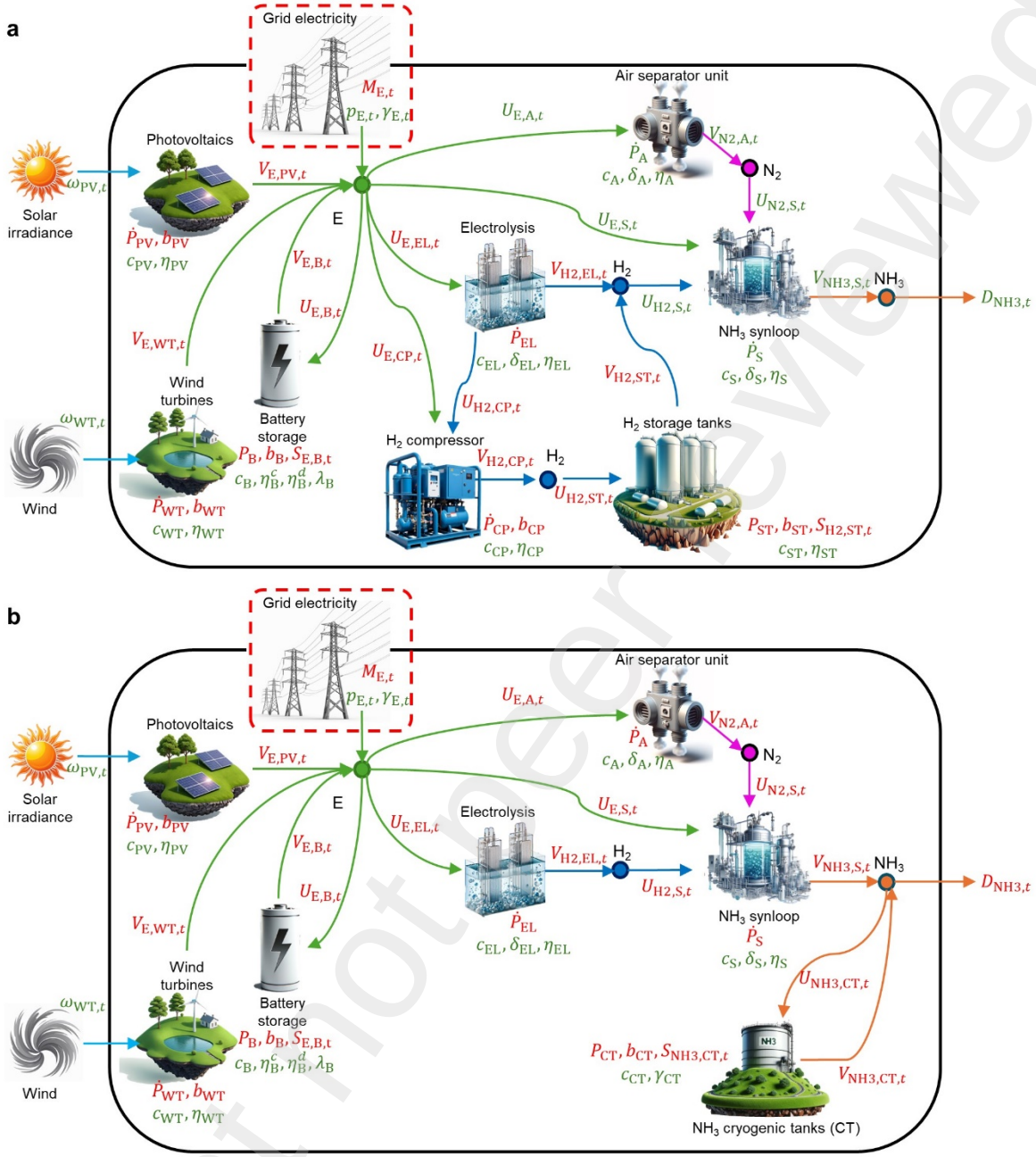

Fig. 1: Electrolytic ammonia plant subsystems. **a** continuous plant; **b** flexible plant. Variables in red indicate the decision variables of the model, while variables in green are input parameters for the optimization model. Colored lines represent energy carriers: green: electricity (E), purple: nitrogen (N_2), blue: hydrogen (H_2), and orange: ammonia (NH_3). In the semi-islanded mode of operation (red dashed lines), where the plant primarily relies on renewable energy sources yet remains connected to the grid for backup, the import of grid electricity is allowed if it complies with the emission constraints.

2.1. Main subsystems of electrolytic ammonia plants

Despite advancements in process technology, the fundamental chemistry of the HB process has remained largely unchanged since its original development. While different pathways exist for

producing the hydrogen feedstock, such as SMR in today's plants and electrolytic hydrogen in this study, the core components of the plant remain largely unchanged. In modeling semi-islanded electrolytic ammonia plants, we included the following subsystems:

- Renewable power generation: wind turbines (WT) or solar photovoltaic systems (PV) to provide low-carbon electricity to the ammonia production plant.
- Transmission and wiring: Transmission lines and wires are necessary to connect the plant to the electrical grid, PV, and WT.
- Electrolyzers: These devices produce hydrogen through water electrolysis and are the key components of the electrolytic ammonia plant. They are also the most energy-intensive subsystem of the plant [31].
- Air Separation Unit (ASU): This subsystem separates nitrogen from air, which is then combined with the hydrogen produced by the electrolyzers to form ammonia.
- Ammonia synthesis loop (Synloop): The ammonia synthesis loop, or HB reactor, is where ammonia is synthesized with an iron-based catalyst. It includes compressors, heat exchangers, ammonia converters, and liquefaction.
- Ammonia storage: Ammonia plants usually incorporate atmospheric pressure ammonia storage facilities that store up to two weeks of production.

These core components are necessary to produce electrolytic ammonia, although their specific configurations may differ based on the unique characteristics of each plant, such as plant size and desired production flexibility. For example, small plants might use different types of ASU; however, there will still be an ASU as a key component of the plant. It is also important to consider the size of the ammonia plant when selecting appropriate technologies, as different solutions may be more appropriate for different scales of production. In large-scale ammonia plants, cryogenic ASUs are typically used for purifying nitrogen. However, other separation technologies, such as pressure swing adsorption (PSA), may be more appropriate for smaller-scale plants due to their higher flexibility and lower cost at small scales [31,32].

In addition to the main components reported above, additional systems and equipment might be present depending on the plant's specific design and operating conditions.

- Compressor for hydrogen surplus (in case of a continuous plant): to compress and store any excess hydrogen produced by the electrolyzers to offset fluctuations in renewable power generation.
- High-pressure (350 bar) hydrogen storage tanks (in case of a continuous plant): to provide storage capacity for hydrogen.
- Battery Energy Storage Systems (BESS): to store excess electricity generated by renewable power sources or to provide backup power in case of grid outages.
- Additional cryogenic tanks for ammonia storage (in case of a flexible plant): to produce ammonia during periods of high renewable capacity and store it for later use.

A detailed description of the subsystems is provided in section 0.

2.1.1.Modeling a continuous plant

In the continuous plant layout (**Fig. 1a**), the ammonia plants operate non-stop, ensuring an uninterrupted ammonia output, $V_{\mathrm{NH3},S,t}$ of approximately 42 t NH_3/h (equivalent to 1,000 t NH_3/d [33]) (*eq. 3*). To maintain this constant ammonia output, a continuous supply of hydrogen $U_{\mathrm{H2},S,t}$ is required for the synloop (*eq. 4*). A constant hydrogen supply can be ensured in multiple ways. Grid electricity can be used to produce hydrogen when renewable energy sources are not available while complying with

emission constraints. Additionally, BESS can be installed to store energy and use it at moments of energy shortage to maintain steady-state plant operations. Moreover, the energy surplus from peak renewable hours can be used to produce a hydrogen surplus. This hydrogen can be compressed, stored in high-pressure tanks, and used later in moments of energy shortage.

$$V_{NH3,S,t} = D^{h}_{NH3}, \forall\, t \in \{0, ..., T\} \quad \textit{eq. 3}$$

$$U_{H2,S,t} = V_{H2,EL.t} - U_{H2,ST,t} + V_{H2,ST,t}, \forall\, t \in \{0, ..., T\} \quad \textit{eq. 4}$$

Where D^{h}_{NH3} is a constant representing the amount of ammonia that must be produced each hour of the year; $V_{H2,EL.t}$ is the hourly hydrogen output of the electrolyzer; $U_{H2,ST,t}$ is the volume of hydrogen entering the storage tank, and $V_{H2,ST,t}$ is the hydrogen discharged from the storage tank in hour t.

2.1.2. Modeling a flexible plant with variable output

There is no unique definition of the flexibility of an ammonia production plant since its interpretation can vary depending on the context and perspective. This paper provides our interpretation of flexibility considering its different dimensions at both the subsystem and plant levels.

At the subsystem level, flexibility is a technology's capability to operate at a low nominal load and adjust its operations rapidly. In ammonia production plants, this can be accomplished through both technological advancements and system improvements. Technological advancements can include developing new materials or hardware improvements that enhance the technology's dynamics. For instance, the introduction of innovative catalysts in the HB process permits operations at reduced temperatures and facilitates quicker ramp rates. Conversely, advancements in system and process engineering can achieve similar fast ramp rates and low minimum loads by adjusting the process to a more intermittent energy supply. An example is nitrogen production, where deliberately expelling surplus nitrogen while operating the ASU can attain a minimum load of 10%. This method effectively lightens the load on other subsystems without significant energy waste, thanks to suitable system control.

At the plant level, flexibility is the capacity to adjust output throughout the day, seamlessly following the input energy from renewable energy sources. The greater the ability to adapt to variable input energy, the greater the flexibility. The plant's flexibility level is tied to the least flexible technology, implying that any constraints on such technology's output or load capacity will limit all other systems.

In this paper, discussions on flexibility encompass both aspects. We do not differentiate between subsystem-level advancements and plant-level improvement, as the distinction does not influence our results.

Due to the variability in the flexibility of ammonia synloop and air separation unit subsystems [6,21,31], we propose two distinct scenarios: (i) a semi-flexible scenario with a minimum load of 50% of the nominal capacity for ASU and synloop and (ii) a fully-flexible scenario with a minimum load of 10%, as described in sections 2.2.7 and 2.2.8.

The annual ammonia production, D^{y}_{NH3}, is the same for both the flexible and continuous plants (365,000 t NH_3/y), but the flexible plant operates dynamically to produce ammonia during periods of high renewable energy supply and eventually stores it in additional ammonia storage tanks for periods of low renewable energy supply (**Fig. *1*1b**). This reduces or eliminates the need for hydrogen compressors and storage but may require additional ammonia storage capacity. Unlike the continuous plant, in the flexible plant layout, we also optimize the hourly output of ammonia, $D^{h}_{NH3,t}$ as a decision variable**eq**.

55. The flexibility of the plant operation enables it to adjust ammonia production in response to changing renewable energy supply and demand and potentially reduce overall LCOA.

$$\sum_{t=0}^{T} D^{h}_{NH3,t} = D^{y}_{NH3} \qquad \textit{eq. 5}$$

where the hourly output of ammonia, $D^{h}_{NH3,t}$ is equal to the output of the ammonia synloop, $V_{NH3,S,t}$, minus the ammonia entering the cryogenic storage, $U_{NH3,CT,t}$, plus the output of ammonia from the storage $V_{NH3,CT,t}$ (*eq. 6*).

$$D^{h}_{NH3,t} = V_{NH3,S,t} - U_{NH3,CT,t} + V_{NH3,CT,t}, \forall\, t \in \{0, \ldots, T\} \qquad \textit{eq. 6}$$

2.2. Input parameters to the optimization model

Table 1 presents all the input parameters used in our model. The ranges for these parameters are based on values found in Europe and provide relevant insights for the region. Note that we assume to install all components in 2025 and start operations on January 1, 2026, until December 31, 2050 (lifetime, L, of 25 years).

Table 1: Input parameters for the optimization model, including generic input parameters, technology input data, and grid input data. The ranges from pessimistic to optimistic values were used for the sensitivity analysis, while the reference values were employed for the main analysis.

Input parameter	Description	Unit	Value			Note	Source
			Pessimistic	Reference	Optimistic		
Generic input data							
D^{y}_{NH3}	Annual ammonia production	t NH3/y	365,000				[33,34]
t	Hours/year	h	8,760				
l	Lifetime EHPS	y	25			26 years lifetime, 25 years operations	[33]
r	Discount rate	%	3%	8%	15%		[33]
p_{land}	Agricultural land price	EUR/m^2	15.02	5.86	0.25		[35]
ε_{H2}	Carbon emission limit	kg CO_2e/kg H_2	1				[36,37]
Technology input data							
c_{PV}	Total system cost utility-scale PV	EUR/MW	1,500,000	650,000	400,000		[38,39]
A_{PV}	Total land area for PV installations	m^2/MW	35,000				[40–42]
v_{PV}	Annual O&M	EUR/MW/y	17,000				[6]
η_{PV}	Efficiency PV system	%	90.0%			Considering inverter, transformers, and rectifier efficiencies	[43]
γ_{PV}	Carbon emission PV manufacturing	t CO_2e/MW	787				[44]
c_{WT}	Total system cost utility-scale WT	EUR/MW	1,800,000	1,100,000	850,000		[38,39]

A_{WT}	Total land area for WT installations	m^2/MW	150,000				[40–42]
v_{WT}	Annual O&M	EUR/MW	25,000				[6]
η_{WT}	Efficiency PV system	%		93.0%		Considering transformers, and rectifier efficiencies	[43]
γ_{WT}	Carbon emission WT manufacturing	t CO_2e/MW	1,345				[44]
c_{EL}	Total system cost ALK electrolyzer	EUR/MW	2,100,000	1,700,000	1,300,000	Considering the replacement of two additional stack components during the lifetime of the plant at 100 EUR/kW each	[45]
v_{EL}	Annual O&M	% CAPEX	3.0%				[6]
$\eta_{H2,E,EL}$	Energy demand ALK electrolyzer	kWh/kg H_2	52.0				[46,47]
δ_{EL}	Minimum load ALK electrolyzer	%	10%				[48,49]
γ_{EL}	Carbon emission ALK electrolyzer manufacturing	t CO_2e/MW	133				[50,51]
c_{CP}	Unit cost utility-scale H2 compressors	EUR/kg H_2 compressed per h	11,000				[47]
v_{CP}	Annual O&M	% CAPEX	2.0%				[6]
$\eta_{H2,E,CP}$	Energy demand compressors	kWh/kg H_2 compressed	2.0				[47]
γ_{CP}	Carbon emission H_2 compressors	kg CO_2e/kg compressed per hour	182				[51]
c_{ST}	Unit cost H2 storage tanks	EUR/kg H_2 stored	500				[47]
v_{ST}	Annual O&M	% CAPEX	1%				[6]
γ_{ST}	Carbon emission H_2 storage tanks	kg CO_2e/kg capacity	182				[51]
c_B	Unit cost utility-scale Li-ion battery system	EUR/MWh	735,000	555,000	430,000	Considering two battery packages replacements during the lifetime of the plant	[52]
v_B	Annual O&M	% CAPEX	2.5%				
η_B^c	Charging efficiency	%	92.7%			Round trip efficiency 85%	[52]
η_B^d	Discharging efficiency	%	92.7%				[52]
τ_B^c	Min # time intervals for full charge	n	4				[52]
τ_B^d	Min # time intervals for full discharge	n	4				[52]
λ_B	Self discharge coefficient	% / day	0.2%				[53]
γ_B	Carbon emission Li-ion batteries manufacturing	t CO_2e/MWh	89				[54]
c_A	Total system cost ASU	EUR/MW	9,000,000				[31,55]
v_A	Annual O&M	% CAPEX	2.0%				Assumed
$\eta_{N2,E,A}$	Energy demand ASU	kWh/kg N_2	0.12				[46]

δ_A	Minimum load ASU	%	80%	50%	10%	10% for fully-flexible; 50% for semi-flexible	[9,17]
c_S	Total system cost Synloop	EUR/MW	6,000,000				[31,56–58]
v_S	Annual O&M	% CAPEX	2.0%				[6]
$\eta_{NH3,E,S}$	Energy demand Synloop	kWh/kg NH_3	0.60				[47]
δ_S	Minimum load Synloop	%	80%	50%	10%	10% for fully-flexible; 50% for semi-flexible	[9,18]
c_{CT}	Unit cost NH3 cryogenic storage tanks	EUR/t NH_3 stored	1,000				[31,47]
v_{CT}	Annual O&M	% CAPEX	1%				[6]
d	Distance from PV, WT, grid connection and EHPS	km	5				Assumed
η_{HVLV}	Efficiency transformer from HV to LV	%	99.0%				[43]
η_{LVHV}	Efficiency transformer from LV to HV	%	99.0%				[43]
η_I	Efficiency inverter	%	97.0%				[43]
Grid input data							
p_E	Price grid electricity for industrial user	EUR/MWh	235	105	41		[59]
γ_E	Carbon intensity grid electricity	kg CO_2e/MWh	230	81	3		[60]
η_E	Transmission losses from grid	%	6%			Considering transformer and rectifier efficiencies	[43]
c_{HVLV}	Transformer (from LV to HV) total installed cost	EUR	14,000,000				[12]
c_{LVHV}	Transformer (from HV to LV) total installed cost	EUR	33,000,000				[12]
c_{HVAC}	HVAC transmission line cost	EUR/km	1,600,000				[12]
$p_{E,N}$	Percentage of the original purchase price at which electricity is sold back to the grid	%	0%	25%	100%		Assumed

2.2.1. Renewable resources

To optimize the design and operations of the plants, we utilize historical capacity factors for solar and wind energy generation derived from the Copernicus Climate Change Service (C3S) dataset [61]. C3S offers climate and energy indicators specific to the European energy sector. This includes information on climate-related variables such as solar radiation and wind speed, as well as energy indicators like electricity demand and renewable power generation.

The C3S dataset provides hourly solar and wind capacity factors for the 1979-2022 period for all European regions at NUTS-2 level (**SI - Fig. i**). However, due to computational constraints associated with simulating all potential climate conditions and considering the high temporal resolution of the data, we select representative regions.

Firstly, we calculate the mean annual capacity factor $\overline{\omega}_{k_R,i,j}$ for each region i and year j for both set of renewable energy technologies $\mathcal{K}_R$ $\{PV,WT\}$ according to *eq. 7*.

$$\overline{\omega}_{\mathrm{k_R,i,j}} = \frac{\sum_{\mathrm{t=0}}^{\mathrm{T}} \omega_{\mathrm{k_R,i,j}}}{\mathrm{T}}, \forall\, \mathrm{k} \in \mathrm{K_R} \qquad \textit{eq. 7}$$

We cluster European regions based on a specific set of rules relating to their capacity factors for solar and wind energy. High-capacity factor regions fall into the top 75th percentile for either solar or wind mean annual capacity factors, while also having a mean annual capacity factor greater than the 25th percentile for the other energy source. Solar-dominated regions rank in the top 25th percentile for solar energy capacity but fall into the lowest quartile for wind energy. Wind-dominated regions are in the top 25th percentile for wind energy capacity but in the lowest quartile for solar energy. Median-capacity regions have both solar and wind resources exceeding the 25th percentile but less than the 75th percentile, indicating a balanced mix of both energy sources. Low-capacity regions have one of the energy sources (either solar or wind) with a mean annual capacity factor below the 75th percentile, and the other energy source has a mean annual capacity factor below the 25th percentile, indicating limited potential for renewable energy.

We then select regions with the highest, median, and lowest mean annual capacity factors for both wind and solar installations to create five "representative regions" that represent extreme weather scenarios (**Fig. 2**). These categories include (i) Wind-dominated, (ii) Solar-dominated, (iii) Low-capacity, (iv) Median-capacity, and (v) High-capacity (both solar and wind). More specifically, we identify UKE4 (West Yorkshire, United Kingdom) as a wind-dominated region, showing the highest mean annual capacity factor at 51.5% (99.2nd percentile) specifically for wind, yet it has a relatively poor solar energy capacity, with a factor of just 8.7% (1.5th percentile). Conversely, TRB2 (Van Subregion, Turkey) is an example of a solar-dominated region, with a high mean annual solar capacity factor of 18.9% (99th percentile), while its wind energy capacity trails significantly with a capacity factor of merely 8.7% (3.9th percentile). These selections are made intentionally to represent regions with a strong prevalence of one energy source, wind or solar, while having limited potential for the other. In contrast, TR10 (Istanbul Subregion, Turkey) emerges as a high-capacity region, landing in the 75th percentile for solar energy and the 77th percentile for wind energy, making it unique as most regions tend to excel in only one energy source. Lastly, NO05 (Vestlandet, Norway) and AT12 (Lower Austria, Austria) represent regions with low and median-capacity factors, respectively (**Fig. 2**)

This approach allows us to capture the variability and extremities of climate conditions, while mitigating the computational intensity associated with simulating every year and region in the dataset. At the same time, it ensures the derived information remains valuable and applicable to other regions falling within similar clusters, thereby maintaining its relevance across a broader geographical context (**SI - Fig. ii**).

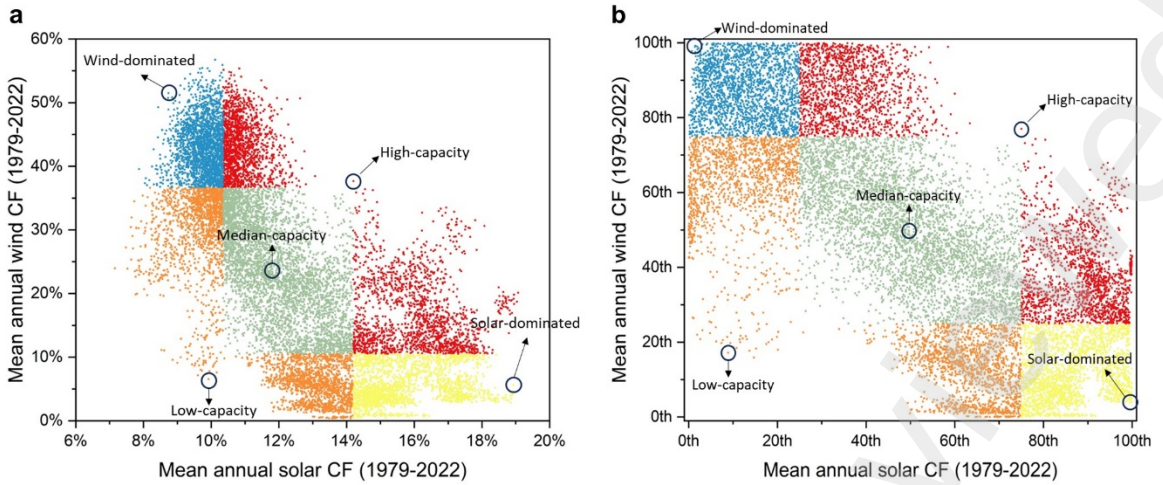

Representative regions	NUTS-2	Year	Avg annual CF PV	Percentile Solar	Avg annual CF WT	Percentile Wind
Median-capacity	AT12	2015	11.8%	49.6	23.4%	49.8
High-capacity	TR10	2001	14.2%	75.0	37.7%	77.0
Low-capacity	NO05	1985	9.6%	8.9	7.1%	17.2
Solar-dominated	TRB2	1995	18.9%	99.9	8.7%	3.9
Wind-dominated	UKE4	1998	8.7%	1.5	51.5%	99.2

Fig. 2: Clustering of European regions at the NUTS-2 level according to their average yearly capacity factor, showcasing the five representative regions and years chosen for analysis. In the scatter plot, each point denotes the capacity factor of each NUTS-2 region and year (from 1979 to 2022) considered in the dataset. The capacity factor is displayed as a percentage in panel **a** and as a percentile rank for each region and year in panel **b**. NUTS-2 is a standardized geocode for subdividing countries in the European Union into regions for statistical purposes. UKE4: West Yorkshire, United Kingdom; TRB2: Van Subregion, Turkey; TR10: Istanbul Subregion, Turkey; NO05: Vestlandet, Norway; AT12: Lower Austria, Austria.

2.2.2. Renewable power generation

To maximize the utilization of local renewable resources, we assume installing a hybrid renewable power generation system comprising utility-scale solar PV and onshore wind turbines. We obtain cost and performance data from the IRENA database [38]. This database includes detailed information on various components, including, among others, the balance of system, transformers, grid connection, wiring, and power electronics. It also provides the weighted average 5th percentile and 95th percentile total system costs for utility-scale wind and solar installations globally.

Given the long lifespan of solar PV and WT, we assume the infrastructure will not be replaced during the projection period 2025-2050 and only consider the 2025 costs. As the IRENA dataset offers data updated only until 2020, we collect IRENA's 2030 cost projections for solar PV and wind turbines from an additional source [39]. To estimate 2025 costs, we assume a linear decrease in costs from 2020 to 2030 using available data. A linear cost reduction is a simplification, considering the historical non-linear drop in costs, but provides a reasonable approximation for short-term cost reduction.

Since the modeled plants are not linked to a specific geographic location but rather represent generalized plants located in Europe, for coherence with capacity factor data (see section 2.2.1), we consider the entire range of costs across Europe provided by the dataset: 400,000 EUR/MW - 1,500,000 EUR/MW, with 650,000 EUR/MW being the reference value (**Error! Reference source not found.**). Similarly, we consider the cost of wind turbines ranging from 850,000 EUR/MW to 1,800,000 EUR/MW, with

the reference value being 1,100,000 (**Error! Reference source not found.**). These values represent the range of utility-scale renewable installation total installed costs in Europe.

Large installations of renewable power generation (GW-scale) are required to power an electrolytic ammonia plant. Hence, we also include in the cost analysis the cost of land. PV systems typically require 3.5 hectares per MW installed, and WT demands about 15 hectares per MW [40–42]. For accurate land cost assessment, we collected price data from the European Commission [35] and calculated the average land price in Europe (~58,000 EUR/ha). However, not all the land will be completely covered by renewable installations. In fact, the 'direct land consumption' is 7% for wind turbines and 86% for solar PV [40–42]. Hence, we multiply the cost of land by only the percentage of direct land used by the renewable installations.

Additionally, our analysis also incorporates electrical losses incurred during the transmission of electricity from PV arrays and WT to the ammonia plant. We assume the construction of new, dedicated transmission lines separately from existing grid infrastructure to avoid the risk of grid congestion during peak production hours. Assuming that the renewable energy installations are located within a short distance (< 5 kilometers) from the plant, we consider High Voltage Alternating Current (HVAC) [62]. Wind turbines typically produce Low Voltage Alternating Current (LVAC), which necessitates stepping up to HV using transformers. This HV power is then transmitted to the plant, where it is stepped down and converted to Low Voltage Direct Current (LVDC) via rectifiers for use. On the other hand, PV systems generate LVDC directly. This necessitates an additional conversion step to transform LVDC to LVAC, before stepping up the voltage for integration into the dedicated HVAC line. It is important to note that the costs associated with inverters required for this conversion in PV systems are already accounted for in the IRENA dataset. Additional costs and losses due to transformers, wires, inverters, and rectifiers are detailed in **Table 1**. The total transmission losses from wind turbines to the electrolysis hydrogen system are estimated at around 7%, with 2% attributed to transformers and 5% to the rectifier [43]. For PV systems, the total transmission losses are around 10%, comprising 3% inverter losses, 2% transformer losses, and 5% rectifier losses [43].

The hourly power generation from PV and WT systems, based on the availability of renewable resources, along with the constraints on installed capacity, are presented in *SI – eq. iv* and *v*.

2.2.3. Grid electricity costs and emissions

Grid electricity can complement renewable sources by reducing the need for larger installed capacity and associated costs, particularly in regions with low-capacity factors [12–14]. Hence, we propose a semi-islanded configuration for the ammonia plants, where we allow the use of grid electricity as a backup. The optimization model determines the optimal amount of imported electricity, denoted as $M_{\mathrm{E},t}$, for each hour, while considering a constraint that limits the maximum amount of imported grid electricity to meet the hourly demand of the plant.

Nevertheless, the reliance on grid electricity results in carbon emissions [12,14]. Recent efforts to identify emission thresholds for electrolytic ammonia to be considered a sustainable chemical focus on the carbon content of the hydrogen utilized in ammonia synthesis. Low-carbon ammonia production should rely on hydrogen derived from 100% or nearly 100% renewable energy, resulting in close to zero operational carbon equivalent emissions [37]. Previous studies [36,37] suggest that an emission limit of 1 kg of CO_2e per kg of H_2 is a cost-effective cap for electrolytic hydrogen in ammonia production in Europe, and we adopt this benchmark for this study. This implies we can import grid electricity as long as the lifespan average emissions of hydrogen do not exceed the 1 kg CO_2e/kg H_2 limit (*eq. 8*).

$$\sum_{l=0}^{L}\sum_{t=0}^{T}\gamma_E M_{E,t} \leq \varepsilon_{H2}\left(\sum_{l=0}^{L}\sum_{t=0}^{T}U_{H2,S,t}\right) \quad \textit{eq. 8}$$

Where γ_E is the carbon intensity of grid electricity in kg CO_2e/kg H_2, while ε_{H2} represents the emission threshold implemented of 1 kg CO_2e/kg H_2. $U_{H2,S,t}$ is the hourly hydrogen input of the ammonia synloop.

To calculate the reference carbon intensity of grid electricity and establish the range for sensitivity analysis, we use the JRC-COM-NEEFE (National and European Emission Factors for Electricity Consumption) from the European Commission [60] for historical data (1990-2020). We assume that all electricity grids will achieve carbon neutrality (zero kg CO_2e per MWh) by 2050, employing a linear reduction approach from the present day to 2050. We then compute minimum, 5th percentile, mean, 95th percentile, and maximum values for each year. We subsequently calculate the average of each percentile from 2026 (the year the facility would be operational) to 2050. As per this, we use 81 kg CO_2/MWh as a reference value and the range 3 – 230 kg CO_2/MWh for the sensitivity analysis (**Table 1**).

Regarding electricity prices, both short-term fluctuations and long-term trends are challenging to predict and lie beyond the scope of our current study. To establish the price range, we collect historical electricity prices for large-scale industrial users from a dataset compiled by the European Commission [59]. This dataset includes country-based monthly historical electricity prices for industrial users from 2008 to 2019. Electricity prices in Europe exhibit great variability, ranging from 41 EUR/MWh to 235 EUR/MWh, with 105 EUR/MWh as the reference value (**Table 1**).

Since the plant is connected to the national electricity network, we also consider the possibility of selling excess renewable electricity back to the grid instead of curtailing it [12]. Salmon & Bañares-Alcántara have shown that when an ammonia plant acts as both a consumer and a supplier to the national electricity network, it can reduce costs [12]. Furthermore, in the future, integrating large-scale electrolytic ammonia plants with domestic electricity markets may simplify the challenges of achieving local grid stability.

Modeling the sale of excess electricity to the grid requires careful consideration of several factors. One key issue is that the plant's surplus electricity production during peak renewable output often coincides with times when the grid may already be dealing with an oversupply. This can lead to reduced demand for additional electricity, with the potential for electricity prices to drop, even becoming negative, as has been observed in several European regions during periods of excess supply [63,64]. The increasing share of renewable energy sources in the energy mix has a significant impact on daily fluctuations in grid electricity prices. Research suggests that these fluctuations escalate as the proportion of renewable energy on the grid increases [65]. Historical data supports this: countries with higher percentages of renewables tend to experience wider average daily fluctuations. For instance, in 2022, Finland and Sweden recorded a 55% and 52% difference, respectively, between the minimum and mean price of electricity, compared to the EU average of 24%.

Given the global trend towards increased incorporation of renewables into energy mixes [66], we can anticipate more prevalent price fluctuations in the future. As ammonia plants would likely sell surplus electricity during periods of excess renewable energy and considering the projected increase in renewable-based grids, we can reasonably expect that the electricity sold would be at a significantly lower price than the average purchase price. We therefore assume that the plant will sell electricity at 25% of the average daily price. However, recognizing the inherent uncertainties, we further investigate this in the sensitivity analysis, testing a "sellback coefficient" ($p_{E,N}$) ranging between 0% and 100% to capture potential variability.

We also implement a constraint on the amount of electricity the plant can import and sell to the grid per hour (*SI – eq. vi*). Because we set a constraint on the amount of imported electricity based on the

capacity of transformers and transmission lines, the same constraint applies to exported electricity (~400 MWh). The plant, thus, cannot sell more electricity than the existing infrastructure can handle. Additionally, if grid export is left unconstrained, the model would favor the construction of exceptionally large renewable energy facilities primarily focused on selling electricity to the grid [12]. This approach could inadvertently create a secondary business model subsidizing the electrolytic ammonia plant. However, this scenario poses challenges, including limited availability of land, substantial upfront capital requirements, and market risks associated with being a significant contributor to the national grid. The local grid infrastructure might not be equipped to accommodate a huge influx of energy during peak renewable production hours. Upgrading the grid to handle such significant energy surpluses from the plant poses a complex challenge, especially due to the high costs and logistical issues involved.

When transmitting large quantities of electricity to and from the grid, dedicated transmission infrastructure is essential. Specifically, this involves the installation of new HVAC lines and transformers, which are necessary to convert HV to LV and vice versa at the plant. To account for energy losses during transmission, we have incorporated an increase in the price of delivered and sold electricity, following the methodology described by Salmon and Banares-Alcantara [12]. Additionally, the extra power required to offset these transmission losses results in a corresponding increase in the cost of electricity. Considering that existing plants are typically situated in industrial areas, we assume proximity to a grid connection point within 5 kilometers. Due to this short distance, line losses are considered negligible. Therefore, only the losses from transformers, estimated at 1%, and rectifier losses at the plant, estimated at 5%, are factored into our calculations.

2.2.4. Battery energy storage systems

We collect the cost and performance of utility-scale battery energy storage systems (BESS) considering lithium-ion batteries (LIBs) from the National Renewable Energy Laboratory's (NREL's) 2023 Annual Technology Baseline [52], which summarizes the research conducted by Augustine and Blair [67] and Ramasamy et al. [68]. These studies provide projections for the future costs of BESS, considering all key components such as the LIB pack, inverter, balance of system, installation costs, and other relevant factors.

We consider a LIB with a duration of 4 hours, which represents the amount of time the storage system can discharge at its power capacity before depleting its energy capacity. We assume a round trip efficiency of 86% [52], with losses equally distributed between charging and discharging, and a 15-year lifetime for the LIB pack [69]. At the end of this period, we anticipate the replacement of the LIB pack, which constitutes approximately 50% of the total system cost. We therefore consider projected 2040 costs for the LIB pack replacement. We also consider battery self-discharge, which occurs due to internal chemical reactions taking place when the battery is not charged or discharged. Cole et al. [70] and Kebede et al. [69] have indicated a daily self-discharge rate ranging from 0.1% to 0.3%. For our analysis, we employ a conservative daily self-discharge rate of 0.2% [53]. Cost and performance values are shown in **Table 1**.

The amount of energy stored each hour is calculated as shown in *SI - eq. vii*. Additional constraints related to energy storage are presented in the *SI - eq. viii-xi*.

2.2.5. Electrolyzers

By utilizing water as the input and electricity as the energy source, electrolyzers separate water molecules into hydrogen and oxygen gases. In the context of an electrolytic ammonia plant,

electrolyzers play a pivotal role as the most energy-intensive component, typically accounting for approximately 90-95% of the total energy demand of the electrolytic plant [71].

We consider alkaline electrolyzers (ALK) because of their maturity, especially for larger applications. Furthermore, there is a trend of planning for ALK electrolyzers in numerous large-scale electrolytic plant projects and studies [19,72,73]. Nevertheless, it is important to acknowledge the need for further research and exploration of alternative electrolyzer technologies, including proton exchange membrane (PEM), solid oxide, and membraneless electrolyzers.

We collect data regarding ALK electrolyzer cost and performances from various sources, including the Hydrohub Innovation Program's extensive literature review conducted in 2022 [45]. This review focused on assessing the costs and performance of large-scale (1-GW) electrolytic-hydrogen production systems. The review projects a 50% reduction in electrolyzer system costs between 2020 and 2030. Considering that plants are assumed to install all subsystems in 2025, we thus anticipate a 25% reduction in costs compared to the 2020 data. We therefore consider a total system cost of 1,500,000 EUR/MW (1,100,000 – 1,900,000). To these costs, we added the additional costs for the replacement of two stack components over the 25-year lifetime of the plant, which would account for approximately 100,000 EUR per MW of installed capacity [45]. This replacement cost represents approximately 10% of the total system cost. Routine maintenance is performed on the remaining systems throughout the operational lifespan of the plant.

The equations describing the minimum installed capacity of the electrolyzers, energy input and output, and the constraints on the minimum hourly load are presented in *SI - eq. xii-xv*.

2.2.6. Hydrogen compressors and high-pressure tanks

In the continuous plant layout, excess renewable electricity can be utilized to synthesize hydrogen, which can then be stored for balancing periods. However, since ALK electrolyzers typically operate at lower pressures (ranging from atmospheric pressure to 30 bar), mechanical compression becomes essential to achieve the desired pressure of approximately 350 bar, commonly used for hydrogen storage tanks [74]. Therefore, a compression process is employed to elevate the pressure to the required level for efficient storage. The estimated electricity consumption for compressing hydrogen to this pressure is around 2 kWh/kg H_2 [47]. In terms of investment costs, we assume 11,000 EUR/kg H_2/h for the compressor and 500 EUR/kg H_2 for the high-pressure tank based on the study conducted by Ikäheimo et al. [47].

The amount of hydrogen compressed and stored each hour is described by the equations presented in *SI - eq. xvi-xix*.

2.2.7. Air Separator Unit

Separating nitrogen (N_2) directly from the air can be done through three main methods: (i) cryogenic distillation, (ii) pressure swing adsorption (PSA), and (iii) membrane separation. Among these methods, cryogenic distillation offers the purest product with the lowest specific energy consumption, making it economically advantageous for large-scale electrically-driven ammonia production facilities [46].

Conventional ASUs, and in particular cryogenic distillation units, must operate above a minimum load of 50-70% of the nominal capacity [6,13]. This minimum load requirement ensures efficient operation, maintains product quality, and ensures system safety. However, recent advancements removed such limitation allowing for a minimum load as low as 10% and fast ramp rates [75]. Additionally, current technologies offer an alternative way to overcome the minimum load limitation. By wasting excess

nitrogen when operating the ASU at 50% load, it is possible to achieve a minimum load of 10%. This approach effectively reduces the load on other subsystems without significant energy waste, thanks to appropriate system control.

By enhancing the flexibility of ASUs, grid electricity usage and emissions can be reduced while maximizing the plant's design capabilities. The inclusion of additional buffer storage for nitrogen does not result in a significant increase in ASU capital expenditure, and therefore, it is not considered in our paper's modelling [21].

In the Supplementary Information, *SI - eq. xx-xxiii* present the constraints on the minimum load of the ASU, the equations regulating its hourly input-output, and the constraint on the minimum installed capacity of the ASU.

2.2.8.Ammonia synloop

The HB ammonia synthesis loop comprises several components, such as a synthesis reactor, mixing units, compressors, heat exchangers, and an ammonia separation unit. Operating within a pressure range of 150 to 300 bar and temperatures between 350 to 550°C, these conditions are carefully selected to optimize the reaction rate, considering that the yield per single pass typically ranges from 15 to 25%. The synthesis loops are primarily designed for steady-state operation at near maximum capacity, with limited flexibility for reduced operation due to operational constraints [6].

One of the main challenges in achieving operational flexibility lies in minimizing load variability within the ammonia synthesis loop. The reactor's characteristics limit dynamic operation, necessitating a continuous supply of hydrogen, nitrogen, and process electricity [6]. Leading companies like Topsoe have developed design solutions that enable operation down to 10% capacity [16,76]. Potential solutions to enhance system flexibility include the use of electric heaters to maintain the reactor's temperature profile at low operational loads, variable load compressors to reduce compression rates, and utilizing surplus nitrogen to regulate flows and pressure within the ammonia loop [31].

The constraints on the minimum load of the ammonia synthesis loop, the equations regulating its hourly input-output of hydrogen, nitrogen, and electricity, and the constraint on the minimum installed capacity of the synloop are described in the Supplementary Information, *SI-eq. xxiv-xxviii*.

2.2.9.Cryogenic storage

Cryogenic tanks are specialized containers designed for the storage of ammonia at cryogenic temperatures, usually below -33°C. Cryogenic tanks are extensively employed in ammonia plants and various industries to safely store ammonia, mitigating the likelihood of leaks or environmental hazards until it is required for industrial applications or further processing.

Conventional ammonia plants typically incorporate cryogenic storage tanks with a capacity equivalent to two weeks' worth of ammonia production. However, in the case of a flexible plant layout, we include the possibility of installing supplementary cryogenic storage tanks to serve as a buffer.

Equations *SI – eq. xxix* and *xxx* in Supplementary Information describe how ammonia storage is modeled in the optimization problem. These equations represent the hourly ammonia storage dynamics and the constraints on the storage capacity.

2.3. Carbon emissions analysis

We calculate the operational emissions resulting from the electricity imported from the grid by multiplying the total electricity consumption by the grid electricity carbon intensity and dividing the total carbon emissions by the amount of ammonia produced during the same period (*eq. 8*).

In addition to operational emissions, we also calculate technology-embedded emissions, which are the emissions resulting from the manufacturing and transportation of key plant subsystems, such as PV installations, wind turbines, electrolyzers, battery and hydrogen storage. These embedded emissions γ_k are calculated per unit of installed capacity for each subsystem k, taking into account the emissions associated with the production of raw materials, component manufacturing, and transportation and then multiplied by the installed capacity $\dot{P}_k$ across different regions and plant layouts (Text 1 in SI).

The carbon content per unit of ammonia produced, Γ_{NH3}, accounts for the lifetime operational emissions ($\sum_{l=1}^{L}\sum_{t=1}^{T}\gamma_{\mathrm{E}}M_{\mathrm{E},t}$) resulting from imported electricity from the grid and the lifecycle carbon emissions associated with the installation of each technology. The total emissions are then divided by the lifetime ammonia production to obtain the overall carbon content per unit of ammonia produced (*eq. 12*).

$$\Gamma_{\mathrm{NH3}} = \frac{\left(\sum_{\mathrm{l}=1}^{\mathrm{L}}\sum_{\mathrm{t}=1}^{\mathrm{T}}\gamma_{\mathrm{E}}\mathrm{M}_{\mathrm{E,t}}\right) + \sum_{\mathrm{k}\in\mathrm{K}}\gamma_{\mathrm{k}}(\dot{\mathrm{P}}_{\mathrm{k}})}{\sum_{\mathrm{l}=1}^{\mathrm{L}}\mathrm{D}_{\mathrm{NH3}}^{\mathrm{y}}} \qquad \textit{eq. 12}$$

2.4. Sensitivity analysis

We conduct a comprehensive univariate sensitivity analysis to evaluate the impact of varying input parameters on the optimal design and operation of the ammonia plant. These parameters include the unit cost of solar PV systems, wind turbines, and electrolyzers, as well as the price and carbon intensity of grid electricity. Additionally, we examine the effects of varying the minimum load capacity of the air separator unit and ammonia synloop, along with different prices of electricity sold to the grid. The analysis also takes into account the discount rate applied in the financial calculations. The range of values used in the sensitivity analysis is shown in **Table 1**, along with their reference values used in the main analysis. This analysis allows to assess how changes in these parameters could influence both the LCOA and the carbon content of the produced ammonia, therefore assessing their impact on the plant viability. We perform the sensitivity analysis for all plant setups, namely continuous, semi-flexible, and fully-flexible configurations, and representative regions, namely High-capacity, Median-capacity, Low-capacity, Solar-dominated, and Wind-dominated.

3. Results

3.1. Fully-flexible plants abate costs in all regions

The LCOA for continuous, semi-flexible, and fully-flexible electrolytic ammonia plants across the five representative regions is presented in **Fig. 3**. The highest LCOA is observed in regions with low renewable capacity, where costs range from 2,223 to 2,325 EUR/t NH_3, depending on the plant configuration. In contrast, the lowest LCOA can be found in regions with a strong wind energy presence, especially in flexible plant layouts; here the cost is as low as 762 EUR/t NH_3. These figures align with previous estimates, which generally fall between 750 and 2,500 EUR/t NH_3 [24]. This indicates that except for plants situated in regions with substantial renewable energy potential—particularly those with excellent wind power—electrolytic ammonia is more costly than that produced using SMR. Historically, the LCOA for fossil-based ammonia production typically ranges between 250 and 1,000 EUR/NH_3 [24].

Geographic location and, thereby, the local climate conditions and renewable energy availability strongly affect the optimal design and operation of the plant and, thus, the LCOA. Wind-dominated regions consistently yield the lowest LCOA, regardless of the plant configuration, whether continuous or flexible. These findings suggest that wind power is particularly well-suited to drive the operation of electrolytic ammonia plants. Interestingly, regions with very high wind energy availability (in our study, the 99th percentile) and poor solar resources yield a lower LCOA than regions with both high solar and wind resources but to a lesser extent. In fact, high-capacity factor regions (accounting for both wind at the 77th percentile and solar at the 75th percentile) result in 22%, 23%, and 27% higher LCOA compared to wind-dominated regions in continuous, semi-flexible, and fully flexible plant configurations, respectively. In contrast, solar-dominant regions have significantly higher costs compared to wind-dominant regions, with cost increases ranging from 65% to 88%. Surprisingly, regions with median capacity factors exhibit lower costs than regions relying exclusively on solar energy. This indicates that abundant solar resources cannot compensate for sub-optimal wind resources. On the other end of the spectrum, regions with low-capacity factors necessitate large-scale installations across all subsystems to counter the scarcity of renewable resources. This requirement substantially increases costs, resulting in an LCOA almost three times higher than those observed in wind-dominant regions.

Electrolytic ammonia plants in wind-dominant regions exhibit lower costs due to two key reasons. Firstly, the consistent wind energy in these regions results in less need for a large-scale renewable energy infrastructure, reducing both initial investment and maintenance costs. Secondly, relying on wind power minimizes installing costly energy storage systems and importing grid electricity as a backup. Wind energy is more evenly distributed throughout the day and night than solar power, making it easier for the plant to ensure extended operational hours relying on renewables (semi-islanded), reducing the need for stored power. These findings, consistent with other research [21], highlight the economic benefits of situating such plants in wind-rich regions and the importance of strategic geographic placement for renewable energy-powered facilities.

Another key finding is that the plant configuration, specifically the choice between flexible and continuous operation, can impact costs differently based on the geographical region. In wind-dominated regions and regions with high renewable potential from both solar and wind sources, semi-flexible plants present lower costs than continuous plants, achieving a cost reduction of 6% and 5% respectively. This cost advantage is likely due to the more consistent availability of wind energy, including during the night, which enables the plants to more easily maintain the 50% minimum load required by the ASU and ammonia synthesis loop. Conversely, in solar-dominant regions, a semi-flexible plant layout incurs higher costs than continuous plants, resulting in an up to 7% increase in the LCOA. The challenge here is the intermittent nature of solar power. Since solar energy is not available during the night, it becomes difficult to maintain the 50% minimum load required by the plant without extensive battery storage or grid import, both of which can substantially increase costs. Therefore, in solar-rich regions, it is more

beneficial to opt for a continuous plant configuration rather than a semi-flexible. During peak solar hours, plants can produce and store hydrogen. This stored hydrogen can then be used during the evening hours or other periods when solar power is not available, effectively balancing the energy supply and keeping the plant running at the required load.

Interestingly, the LCOA in regions with median and low renewable energy capacity is similar for both continuous and semi-flexible plants. This suggests that the choice between continuous and semi-flexible operation has less impact on costs in these regions than those dominated by a specific renewable energy source.

Finally, the full potential of flexible plants is realized in the fully-flexible configuration. In this setup, plants have the capability to rapidly reduce their load to a minimum of 10% and subsequently ramp up again as needed. This rapid load adjustment capability allows the plant to closely follow the availability profiles of renewable energy sources. By operating in a fully-flexible configuration, the plant can optimize its operation to coincide with times of high renewable energy availability, thereby reducing the need for stored energy or grid imports. When renewable energy is in abundance, the plant can ramp up its operation, and when renewable energy is scarce, the plant can reduce its operation to a minimum. Given that the energy demand of the ASU is relatively small compared to the plant's total energy demand, possible losses of efficiency due to running at minimum load do not significantly impact overall costs. The ability to rapidly adjust loads in response to renewable energy availability makes the plant more efficient in its use of renewable resources and results in lower costs. This advantage is more pronounced in wind-dominated regions and regions with high renewable potential, with a 12% and 9% cost reduction compared to continuous plants in the same regions, respectively. In both regions, grid imports are minimal, with approximately 2% of the energy used to power the plant sourced from the grid, indicating that production could potentially be accomplished even with off-grid plants (islanded). The smallest cost reduction for fully-flexible plants is again in solar-dominated regions, with only a 1% reduction in LCOA compared to continuous production plants.

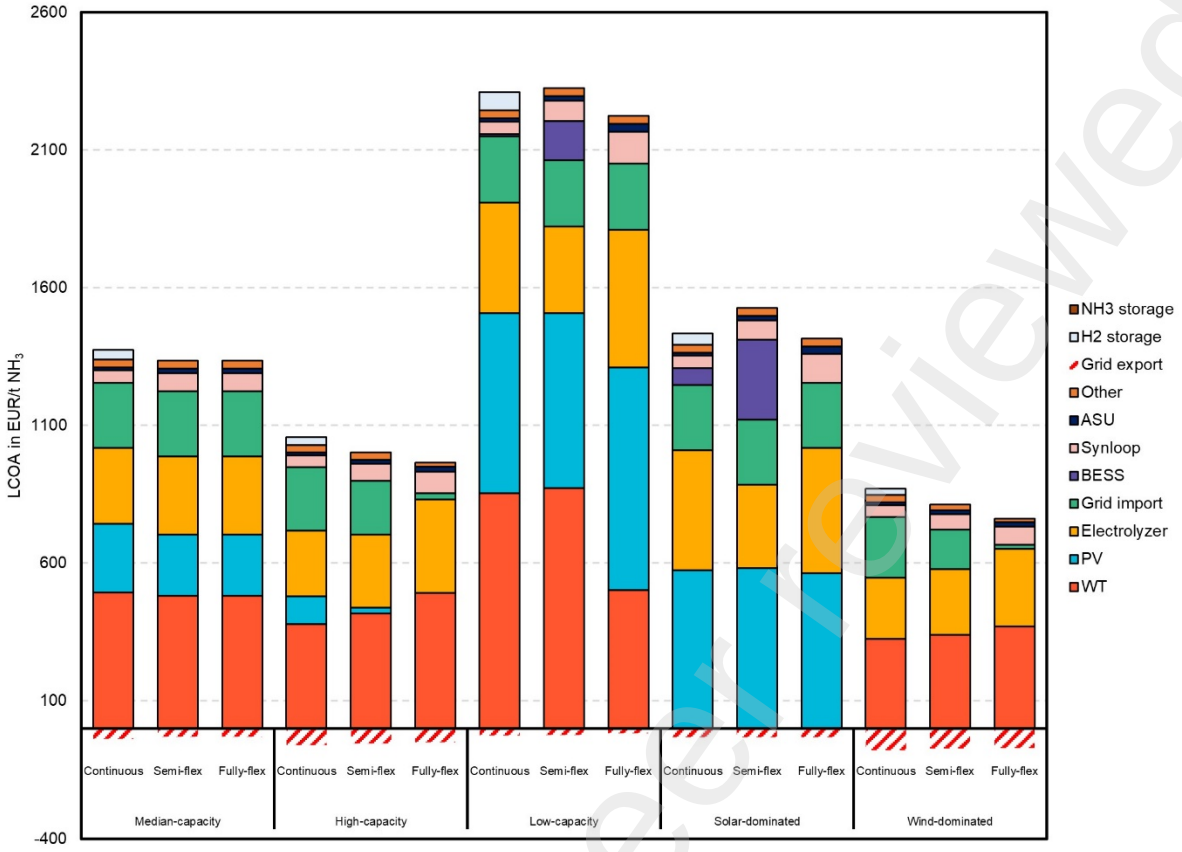

Fig. 3: Levelized Cost of Ammonia (LCOA) for continuous, semi-flexible, and fully-flexible electrolytic ammonia plants in five representative regions, with a breakdown of cost contributions. The selected representative regions are UKE4 (West Yorkshire, United Kingdom), a Wind-dominated region; TRB2 (Van Subregion, Turkey), a Solar-dominated region; TR10 (Istanbul Subregion, Turkey), a High-capacity region; NO05 (Vestlandet, Norway), a Low-capacity region; and AT12 (Lower Austria, Austria), a Median-capacity region. The stacked bar chart illustrates the impact of plant flexibility and plant location on the LCOA and highlights the varying cost components across the different regions.

3.2. ASU and Ammonia synloop minimum load is critical, especially with poor wind

The minimum load capacity of the ASU and ammonia synloop can increase by up to 12% the costs of a flexible ammonia plant. When the minimum load is high, it imposes constraints on other components to match the minimum load requirements of these two subsystems.

Fig. 4 shows the relationship between increasing the minimum load of the ASU and synloop, ranging from 10% to 80% (x-axis), and the LCOA of flexible plants (y-axis). The points marked with black circles represent the break-even points with continuous plants, which are not influenced by the minimum load of the two subsystems. As the minimum load increases, the LCOA also increases. However, this rate of increase is more pronounced in regions with low-capacity factors and less significant in regions with high renewable potential.

In wind-dominated regions, flexible plants require a minimum load of 80% to achieve a lower LCOA compared to continuous plants. This is likely due to the more constant availability of wind energy,

which allows the plant to operate efficiently at this higher minimum load. In these regions, a 10% minimum load results in a 12% cost reduction.

On the other hand, regions dominated by solar energy require a much higher level of flexibility in the plant's subsystems to break even with continuous plants, with a minimum load of about 20%. The reason for this is the intermittent nature of solar power. Because solar energy is not available during the night, it is more challenging to maintain a high minimum load. Therefore, to remain operational and efficient during periods of low or no solar energy, the plant must be able to reduce its load to a much lower level.

These findings help explain why some regions see more significant cost reductions with a fully-flexible plant setup compared to others. In areas with a high renewable potential, particularly those dominated by wind energy, a fully-flexible plant can operate more efficiently and at a lower cost. However, in solar-dominated regions, the advantages of a fully-flexible configuration are less pronounced due to the greater need for flexibility in the plant's subsystems.

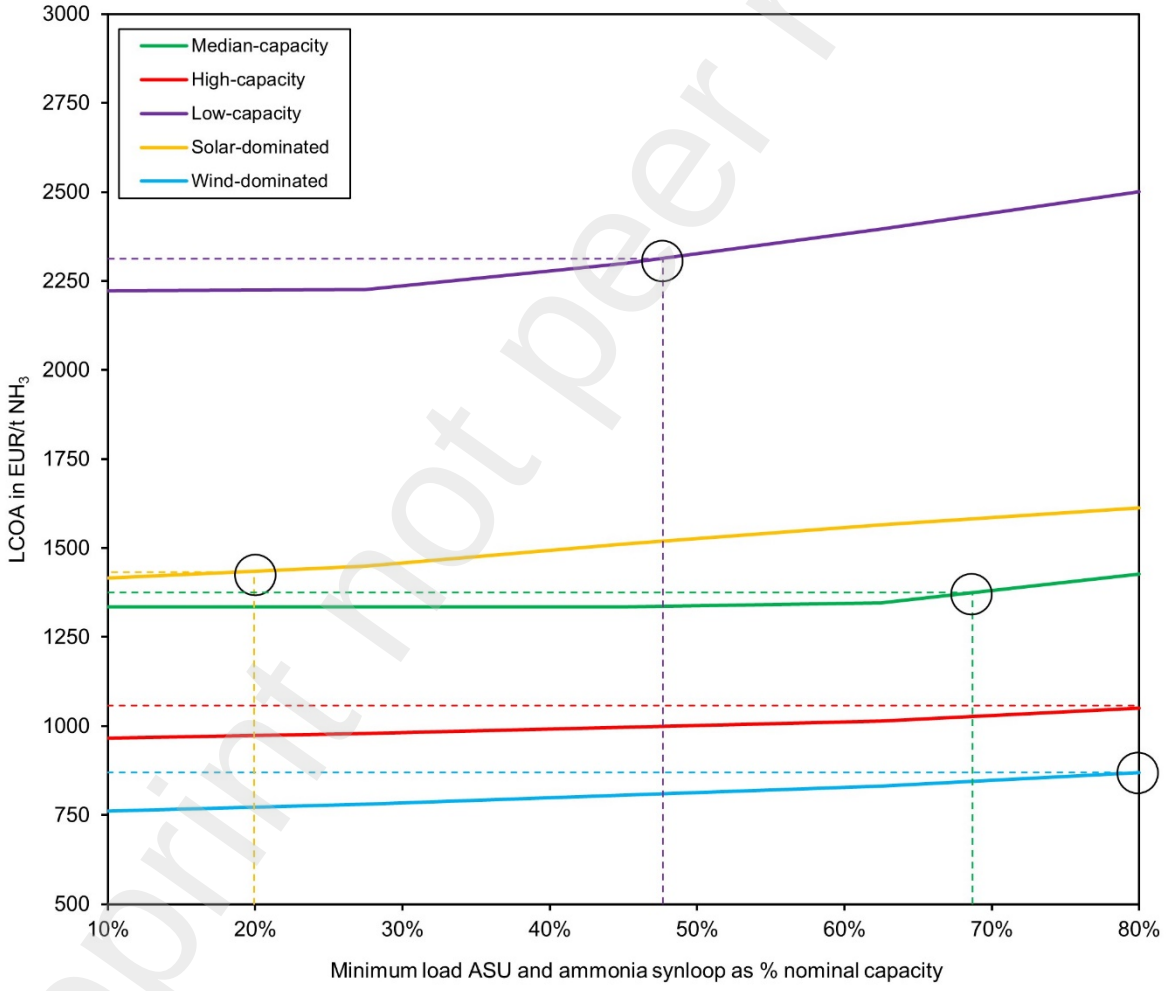

Fig. 4: Effect of Air Separator Unit (ASU) and ammonia synloop minimum load as a percentage of the nominal capacity on the LCOA in flexible plants. Circled points represent the break-even point with continuous plants, which are not affected by the minimum load of ASU and synloop.

3.3. Optimal plant designs

Table 2 presents the optimized design of electrolytic ammonia plants, detailing the installed capacity of various subsystems and the annual electricity exchange with the grid for different plant configurations and flexibility levels across the five representative regions. The optimal plant design and operations can vary significantly among regions and configurations. Regions with low-capacity factors require twice the installed capacity of renewable generation compared to median-capacity regions, and up to five times the installed capacity compared to wind-dominated regions. This means that as renewable conditions worsen in a region, there is a non-linear increase in PV and WT installations.

Regions relying heavily on solar have a total installed capacity of renewables similar to median-capacity regions (around 2.5 GW). However, solar-dominated regions rely exclusively on PV, while median-capacity regions have a more balanced split between PV and WT. In regions characterized by low capacity, continuous plants often see larger renewable installations. Here, the capacity of such installations can range from 4.5 to 5 GW. On the other hand, regions where wind energy is predominant typically feature smaller-scale installations, averaging around 1 GW of wind capacity.

The installed capacity of electrolyzers tends to be homogeneous, ranging from 500 MW to 700 MW for most plants. An exception is fully-flexible plants in low-capacity regions, which require larger electrolyzers to produce sufficient hydrogen during the rare periods of high renewable energy availability. This necessity is also reflected in the larger capacity of the ASU and synloop in these low-capacity regions. In other regions, the installed capacity of ASU and synloop is more homogeneous.

Within the same region, fully-flexible plants typically have the largest ASU and synloop installations. This maximizes their operational efficiency and output due to their ability to harness renewable resources effectively. However, as the cost of these installations is minimal compared to other subsystems, it does not significantly affect the LCOA.

Semi-flexible plants in regions with low wind resources require large battery installations. Specifically, low-capacity regions install up to 1.1 GWh of BESS, while solar-dominated regions install up to 2.3 GWh. This is because plants primarily relying on large solar PV systems generally need BESS to maintain operations or a minimum load during night hours [6]. Therefore, the higher the minimum load, the larger the BESS installed.

Continuous plants in solar-dominated regions have the largest compressors but the smallest storage capacity among continuous plants. This is due to the significant amount of renewable energy that is converted during the day, compressed within a few hours, and stored only for a short duration, typically for use during the subsequent night. This setup does not necessitate long-term hydrogen storage tanks. Conversely, regions with less reliable access to renewable energy sources necessitate larger storage tanks to accommodate hydrogen. This allows for the optimal utilization of renewable energy when it is available and ensures a steady supply of hydrogen during periods of low renewable energy production.

Fully-flexible plants demonstrate a significant reduction in electricity imports, averaging 37% less compared to other plant configurations. By aligning production with renewable energy supply, fully-flexible plants minimize their reliance on grid electricity for balancing periods, resulting in lower grid import requirements. In regions with abundant renewable energy resources, particularly wind, the reduction in grid electricity imports is even more pronounced. Fully-flexible plants in these regions can achieve more than a 90% decrease in grid imports compared to semi-flexible and continuous configurations. This allows them to rely more on their renewable energy sources and minimize dependence on imported electricity. Additionally, regions characterized by high-capacity and wind-dominated configurations often export a greater amount of energy. The increased electricity export in regions with abundant wind resources is not solely due to the high availability of renewable energy but also because wind energy is available throughout the day and night, allowing for consistent generation and potential export of electricity.

Table 2: Optimal design for continuous, semi-flexible, and fully-flexible plants across synthetic regions. $\dot{P}$ stands for installed capacity, EL electrolyzer, B batteries, CP hydrogen compressor, ST hydrogen storage tank, A air separator unit, M_E imported electricity, and N_E exported.

Region	Design	$\dot{P}_{PV}$	$\dot{P}_{WT}$	$\dot{P}_{EL}$	$\dot{P}_{B}$	$\dot{P}_{CP}$	$\dot{P}_{ST}$	$\dot{P}_{A}$	$\dot{P}_{S}$	$\sum_{t=0}^{T} M_{E,t}$	$\sum_{t=0}^{T} N_{E,t}$
	Unit	MW	MW	MW	MWh	t H2/h	t H2	MW	MW	GWh-yr	GWh-yr
	Maximum	3146	2402	949	2293	9	299	10	62	793	1275
Median-capacity	Continuous										
	Semi-flex										
	Fully-flex										
High-capacity	Continuous										
	Semi-flex										
	Fully-flex										
Low-capacity	Continuous										
	Semi-flex										
	Fully-flex										
Solar-dominated	Continuous										
	Semi-flex										
	Fully-flex										
Wind-dominated	Continuous										
	Semi-flex										
	Fully-flex										

3.4. The higher the flexibility, the lower the emissions

The relative contribution of various emission sources to the overall lifecycle CO_2e emissions in the production of electrolytic ammonia varies depending on the specific plant configuration and the regional renewable energy mix. The primary contributors include the manufacturing of wind turbines and solar PV systems, indirect emissions resulting from the use of grid electricity, and, to a lesser extent, the production and disposal of Li-ion batteries used in energy storage systems. Despite wind turbines having higher emissions per installed MW compared to PV systems, their superior capacity factor leads to lower emissions per kWh or unit of ammonia produced, making them a more favorable option in terms of carbon footprint.

Regardless of plant configuration, lifecycle CO_2e emissions are higher in regions with low capacity and lower in regions with high capacity. Regions rich in wind energy resources demonstrate the lowest lifecycle emissions. Specifically, Wind-dominated regions can achieve 11-64% lower lifecycle emissions than regions abundant in solar energy, depending on the specific configurations of the plants (**Fig. 5**). One of the reasons for the lower lifecycle emissions in wind-dominated regions is the reduced need for grid electricity imports, especially with fully-flexible configurations. Plants that rely on wind energy can often generate a more consistent and higher output due to the natural characteristics of wind, particularly in regions where it is abundant and steady. This allows those plants to operate more independently of the grid and minimizes the need to import electricity.

When considering exported electricity, emissions can be completely offset in wind-dominated and high-capacity regions, thanks to the sale of clean electricity to the grid. In regions with a low or median-capacity factor and solar-dominated regions, emissions are on average reduced by 24%, 10%, and 27%.

Overall, despite considerable uncertainty surrounding the lifecycle emissions of all components, semi-islanded electrolytic ammonia production leads to a 72-93% reduction in carbon emissions when compared to SMR, which typically generates approximately 2.7 kg CO_2 for every kg of NH_3 produced. Nonetheless, when we factor in the potential for selling excess renewable electricity to the grid, the carbon emissions associated with electrolytic ammonia production could be further offset over time. In summary, the adoption of electrolytic ammonia production has the potential to significantly reduce the lifecycle emissions of ammonia.

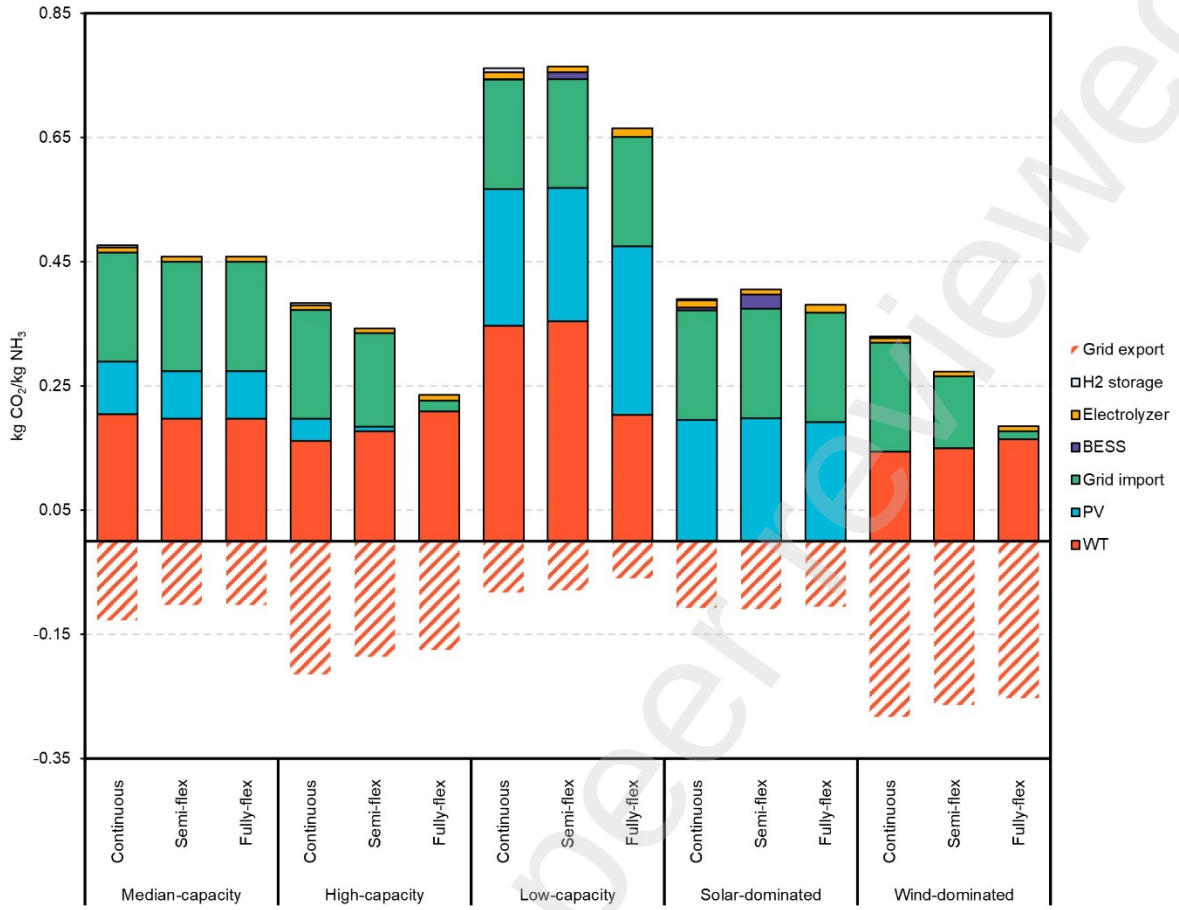

Fig. 5: Average lifecycle carbon emissions per unit of electrolytic ammonia in kg CO_2e/kg NH_3 produced over the lifetime of the electrolytic plant.

3.5. Sensitivity analysis

Fig. 6 presents the sensitivity analysis of the LCOA in five representative regions, exploring the impact of variations in key input parameters. The parameters considered in the analysis include the unit cost of solar PV systems, the unit cost of wind turbines, the price and carbon intensity of grid electricity, the selling price of electricity to the grid, and the discount rate applied in the financial calculations. The figure illustrates how changes in these parameters influence the LCOA, providing insights into the economic viability of electrolytic ammonia production under different input parameter assumptions. By comparing the sensitivity across the five regions, the analysis highlights the relative importance of each parameter and how their impact on the LCOA may vary depending on the specific regional characteristics, such as renewable energy resource availability and market conditions.

The sensitivity analysis reveals that the discount rate is the most influential input parameter on the LCOA (-32%;+84%), with a consistent impact across all regions and plant configurations. This substantial impact highlights the importance of access to affordable capital and favorable financing conditions for the economic viability of electrolytic ammonia projects. Countries with abundant renewable energy resources may face challenges if high costs of capital or difficulties in accessing capital offset the benefits of low-cost renewable energy.

Apart from the discount rate, the impact of other input parameters on the LCOA varies primarily based on the region and its associated renewable energy potential, rather than the specific plant configuration. In fact, plants with similar configurations tend to exhibit comparable responses to changes in input parameters.

Regions with high renewable potential, particularly High-capacity and Wind-dominated regions, show that the price at which electricity can be sold to the grid is the second most influential parameter, with a cost reduction of up to 43% and a cost increase of 9%. This significant impact is due to wind-rich regions exporting the largest amount of energy to the grid, thanks to the more evenly spread availability of wind energy throughout the day compared to solar energy. In contrast, regions with lower renewable potential or those dominated by solar energy may not benefit as much from electricity exports, as the intermittent nature of solar energy limits the amount of excess electricity available. These findings underscore the importance of fostering collaboration among industrial plants with complementary load profiles and the grid. This cooperative approach can optimize the utilization of renewable energy and minimize costs through the sale of excess energy back to the grid.

In High-capacity and Wind-dominated regions, the cost of wind turbines and the price of grid electricity are the next most influential parameters. An interesting result emerges for fully-flexible plants: both low and high costs of electricity lead to a reduction in the LCOA compared to the reference case. When the price of grid electricity is low, the LCOA decreases as expected. However, when the price of electricity is high, the LCOA also decreases. This is because the high price of electricity means that the excess electricity sold to the grid generates significant revenue, reducing the overall costs of ammonia production. The ability to capitalize on high electricity prices by selling surplus energy can significantly improve the economic viability of electrolytic ammonia production, particularly in fully-flexible plants.

The carbon intensity of grid electricity generally has a minor impact on the LCOA compared to other parameters, except for regions with low renewable capacity. In these regions, a clean electricity mix can serve as a valuable alternative to dedicated renewable installations, reducing costs by up to 41% without violating the emission constraint. This finding suggests that in regions with limited renewable energy potential, the availability of a low-carbon grid electricity mix can significantly improve the economic viability of electrolytic ammonia production. By relying on clean grid electricity instead of investing in dedicated renewable installations, projects in these regions can achieve substantial cost reductions while still meeting their emission targets.

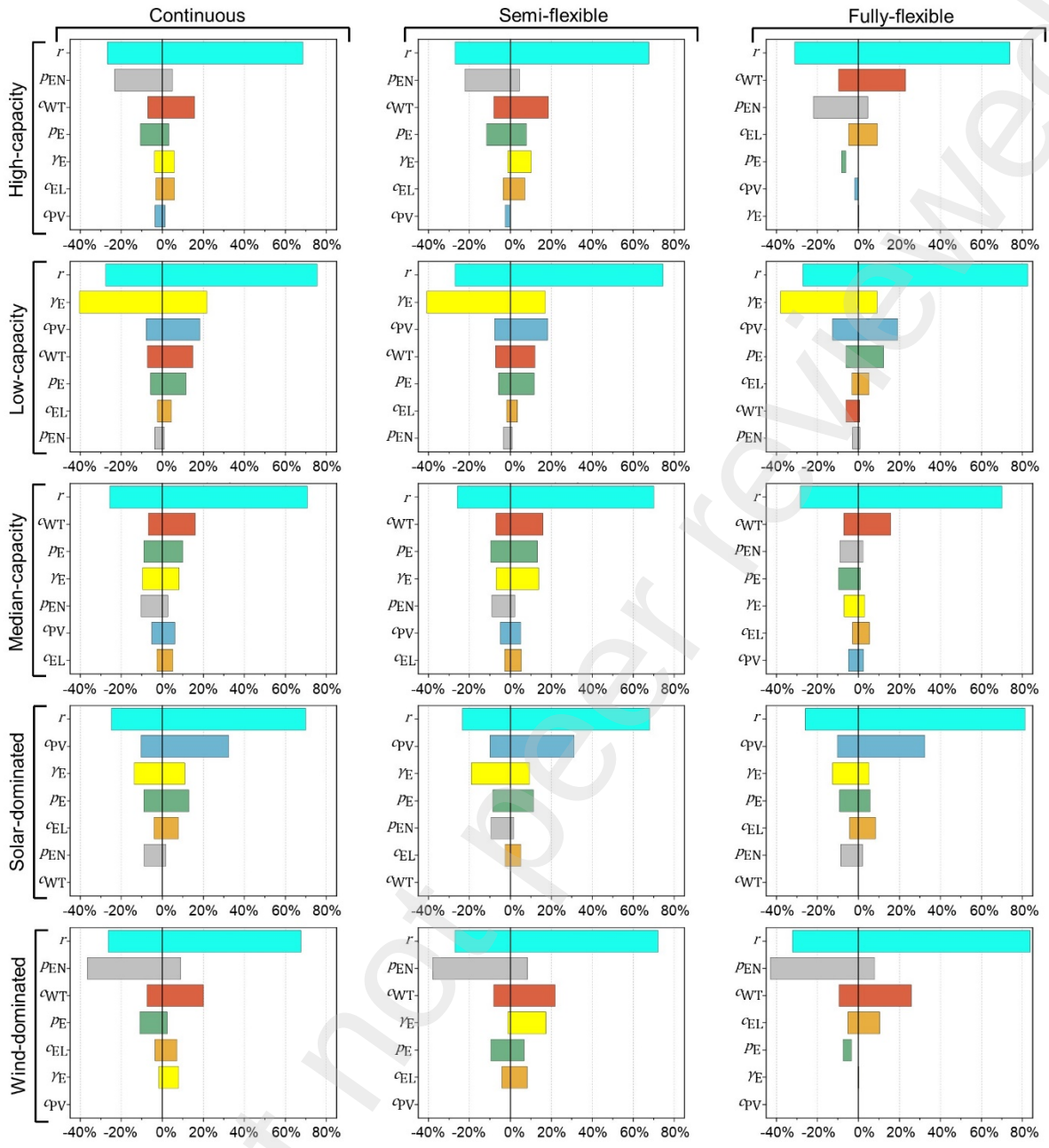

Fig. 6: Sensitivity of LCOA across 5 representative regions. The x-axes represent percentage change compared to the reference case. The y-axes instead represent the range of values used in the sensitivity analysis and reported in Table 1: Discount rate (r, range 3% – 15%), total installed cost of solar PV (c_{PV}, range 400,000 – 1,500,000 EUR/MW), total installed cost of wind turbines (c_{WT}, range 850,000 – 1,800,000 EUR/MW), total installed cost of ALK electrolyzers including replacements (c_{EL}, range 1,500,000 – 2,100,000 EUR/MW), price of grid electricity (p_E, range 41 – 235 EUR/MWh), grid electricity carbon intensity (γ_E, range 3 – 230 kg CO_2e/MWh) percentage of the purchase cost at which excess electricity is sold back to the grid ($p_{E,N}$, range 100% – 0% MWh). The y-axes instead represent the LCOA in EUR/t NH_3.

3.6. The impact of plant flexibility in off-grid plants

Although off-grid (islanded) ammonia plants incur higher costs and require more land for renewable installations, policy interventions like the European Hydrogen Bank [77] initiative or the subsidies for green hydrogen in the US, such as the 45V tax credit [78], could significantly mitigate these costs and enhance the competitiveness of off-grid scenarios. Consequently, we also include an analysis of off-grid plants in our study. This step is crucial to determine whether the conclusions drawn from semi-islanded plants apply to fully off-grid plants.

Our findings align with previous research, which has demonstrated that off-grid (islanded) plants exhibit higher costs compared to their semi-islanded counterparts (SI – Table i). This cost discrepancy is primarily attributed to the oversized renewable installations and storage systems necessary to compensate for periods characterized by suboptimal renewable energy generation. On average, continuous and semi-flexible plants experience a 99% and 110% increase in LCOA when operating in an off-grid configuration, as opposed to a semi-islanded setup. However, the inherent high flexibility of fully-flexible plants enables them to utilize renewable energy sources more efficiently by adjusting production accordingly. Consequently, fully-flexible plants witness only a 19% rise in costs when transitioning from a grid-connected to an off-grid configuration, showcasing their adaptability and cost-effectiveness in various operating scenarios.

4. Discussion

Our research emphasizes that the choice of location is more influential than plant configuration in determining the feasibility and environmental impact of large-scale electrolytic ammonia production. In regions rich in renewable resources, smaller renewable generation infrastructures, grid import, and less reliance on stored energy and hydrogen can yield lower lifecycle carbon emissions and cost per unit of ammonia. This potentially makes electrolytic ammonia competitive with traditional SMR-based ammonia, given historical prices ranging between 250-1000 EUR/t NH_3 [79]. Under favorable renewable conditions, the LCOA could reach approximately 750 EUR/t NH_3, consistent with prior research findings [24]. Near-term policy incentives should concentrate on facilitating the transition from SMR plants to large-scale electrolytic-renewable plants in regions with plentiful renewable resources (especially wind) and sufficient land for installations. Moreover, electrolytic ammonia plants offer substantial environmental benefits, reducing lifecycle carbon emissions by 72%-93% compared to traditional SMR plants, even when utilizing grid power as a backup. The environmental advantage of electrolytic ammonia production becomes even more pronounced when considering the potential emissions offset by selling excess electricity back to the grid or to other industries. Our findings and methods can be further expanded to help define cost-effective lifecycle carbon emission standards of "low carbon" ammonia for specific regions given daily, weekly, monthly, or yearly production needs in the future.

However, electrolytic production in regions with poor renewable potential and stringent land constraints is complex. Here, transitioning to large-scale electrolytic plants could present considerable challenges. For instance, Solar-dominated regions might need approximately 80 square kilometers for solar and wind installations. In contrast, low-capacity regions could require a massive 300-400 square kilometers of PV and wind turbine infrastructure. Despite the potential to repurpose some land used for wind turbines and combine PV installations with agriculture via agro-photovoltaics, substantial land requirements for these renewable infrastructures may limit the possibility of retrofitting current plants in most locations. This highlights how location can dramatically influence not only the economic competitiveness of electrolytic ammonia but also the feasibility of large-scale renewable-based plants. Therefore, careful strategic planning is crucial in the transition towards more sustainable ammonia production.

Our results also brought to light an intriguing observation. Regions with exceptionally high wind energy availability (in the 99th percentile of our study) but poor solar resources, yield a lower LCOA than regions with high but less extreme solar and wind resources. For example, regions with a high-capacity factor (considering wind at the 77th percentile and solar at the 75th percentile) result in a LCOA that is 22% - 27% higher compared to wind-dominated regions depending on the plant configuration. Contrastingly, solar-dominant regions bear significantly higher costs compared to wind-dominant regions, with cost increases ranging from 65% to 88%. Even more surprisingly, regions with median capacity factors exhibit lower costs than regions relying exclusively on solar energy. This finding indicates that abundant solar resources cannot compensate for sub-optimal wind resources.

Fully-flexible plants emerge as the optimal configuration regarding emissions and costs across all regions. Operating at low minimum loads facilitates the full exploitation of local renewable resources, reducing the need for batteries and grid imports, thereby minimizing costs and emissions. This advantage is particularly pronounced in wind-dominated regions. The combination of fully-flexible configuration and abundant wind resources leads to a consistent surplus of electricity production that can be sold to the grid. Since grid export has a significant impact on the LCOA, plants with high-renewable potential can substantially reduce the ammonia price by selling renewable electricity surplus otherwise curtailed. Creating partnerships between industries, ammonia plants, and the local grid is, therefore, a crucial aspect to consider. The potential challenges and opportunities for the co-generation of chemicals and power generation for grid balancing should be explored in future research. Policy instruments could be designed to subsidize a portion of the renewable infrastructure set up by the plant, providing added grid stability. Industries with diverse operational and production requirements can collaborate to develop joint infrastructure, maximizing renewable usage and minimizing energy curtailment. Moreover, results show that achieving very high plant flexibility, with a minimum load of approximately 10% of the nominal capacity, can reduce the cost of ammonia produced in off-grid plants relying exclusively on renewables by an average of 50%. This significant cost reduction is attributed to a much lower reliance of fully-flexible plants on grid energy and a more effective utilization of renewable resources. In light of our findings that fully-flexible plants lead to lower costs, it is clear that enhancing plant flexibility should be a priority for the next generation of large-scale electrolytic plants. The advantages of fully-flexible plants extend beyond economics, as minimizing H2 storage capacity in large-scale plants reduces costs and mitigates safety risks. For example, on May 23, 2019, a hydrogen tank explosion occurred at an alkaline water electrolysis pilot plant facility in Gangneung, South Korea [80], highlighting the potential dangers associated with storing large amounts of hydrogen on-site.

However, despite the promising benefits highlighted, certain obstacles may impede the broader decarbonization of large-scale ammonia plants. One challenge is the substantial capital requirement associated with constructing these facilities. While operational costs tend to decline as more renewables are incorporated, the initial capital investment remains considerable. Depending on the location and plant configuration, these costs can range from 2.5 to 10 billion euros per plant over the anticipated 25-year lifespan. This cost range aligns with estimates for several contemporary projects, such as the REDDAP project in Denmark [19] or the 7-billion project in Morocco [81], showcasing the financial commitment required to transition towards electrolytic ammonia production. This capital-intensive nature can pose difficulties for developing countries abundant in renewable resources, as such nations often lack the necessary capital to invest in large-scale projects. Additionally, these countries could face further challenges due to the higher cost of capital, which can exacerbate the financial hurdles and make the transition to sustainable ammonia production even more challenging. Furthermore, geographical constraints such as access to renewable energy sources, suitable land availability, and proximity to necessary resources and infrastructure present another set of challenges when establishing large-scale plants.

There is an emerging trend toward smaller-scale, decentralized, and off-grid ammonia plants [82]. As underlined by our study, a high level of plant flexibility significantly reduces emissions, costs, and

reliance on grid electricity. Smaller plants have a greater advantage in achieving greater flexibility by utilizing electric compressors and pressure swing adsorption instead of cryogenic distillations as the air separator unit.

While smaller plants may not benefit from the economies of scale characteristic of larger facilities, they present an opportunity to explore innovative approaches to ammonia production. One promising direction is the development of standardized, small-scale modular ammonia plants, where sub-components are organized and manufactured as distinct, standardized building blocks (i.e., modules) that can be easily combined into larger plants and customized to a location's renewable resource profile [82]. This modular design not only simplifies capacity expansion but also offers the potential for cost reductions through standardized production processes and economies of scale in component manufacturing. Furthermore, smaller plants are well-suited for locations with abundant renewable resources, are easier to finance, and bypass the transportation issues associated with centralized larger facilities—issues that can increase costs, emissions, and infrastructure demands. Overall smaller, highly flexible, off-grid ammonia plants, combined with the potential scalability and cost reduction offered by standardized modular designs, form an exciting frontier for future research and development in the ammonia industry. Exploring these possibilities could contribute to transitioning from a fossil fuel-based model to a more sustainable, decentralized ammonia production paradigm. To accomplish this, policy interventions can be instrumental. They can provide targeted funding and incentives for research and development in flexible plant design, support pilot projects in wind-rich regions to demonstrate the viability of these configurations, and foster partnerships between government, academia, and industry to speed up innovation.

5. Conclusions

In this study, we develop a modeling and optimization framework for flexible and continuous electrolytic ammonia plants. We compare different plant layouts, namely continuous, semi-flexible, and fully-flexible configurations, in five representative regions. Large-scale electrolytic ammonia plants provide a promising path for substantial carbon emissions reduction, with the potential to rival the cost-effectiveness of traditional SMR ammonia in areas rich in renewable resources, particularly wind energy. Our research emphasizes the importance of strategic site selection to enhance the economic viability of electrolytic ammonia plants. High plant flexibility not only contributes to lowering the LCOA but also carbon emissions. Our findings and methods will contribute to the definition of future cost-effective lifecycle carbon emission standards for "low carbon" ammonia. Considering the capital intensity of larger-scale electrolytic ammonia plants, small-scale, decentralized settings should be evaluated to support the transition toward low-carbon ammonia production.

Declaration of competing interest

The authors declare no competing interests.

Declaration of Generative AI and AI-assisted technologies in the writing process

During the preparation of this work, the authors used generative artificial intelligence (AI) tools, specifically Grammarly and ChatGPT-4 to enhance language and readability. After using these tools, the authors reviewed and edited the content as needed and take full responsibility for the content of the publication.

Previous versions

The short version of the paper was presented at ICAE2023, Doha, Qatar, Dec 3-5, 2023. This paper is a substantial extension of the short version of the conference paper.

Bibliography

[1] IRENA. Innovation Outlook - Renewable Ammonia. 2022.

[2] Rogers M, Delasalle F, Speelman E, Hoffman J, Shah T, Wuellenweber J, et al. Making Net-Zero Ammonia Possible - An industry-backed, 1.5C-aligned transition strategy. 2022.

[3] Saygin D, Blanco H, Boshell F, Cordonnier J, Rouwenhorst K, Lathwal P, et al. Ammonia production from clean hydrogen and the implications for global natural gas demand. Sustainability 2023;15:1623. https://doi.org/10.3390/su15021623.

[4] Valera-Medina A, Bãnares-Alcántara R, Rouwenhorst KHR, Krzywda PM, Benes NE, Mul G, et al. Techno-Economic Challenges of Green Ammonia as an Energy Vector - Chapter 4. Elsevier; 2020. https://doi.org/10.1016/B978-0-12-820560-0.00001-1.

[5] Smith C, Hill AK, Torrente-Murciano L. Current and future role of Haber–Bosch ammonia in a carbon-free energy landscape. Energy Environ Sci 2020;13:331–44. https://doi.org/10.1039/C9EE02873K.

[6] Wang C, Walsh SDC, Longden T, Palmer G, Lutalo I, Dargaville R. Optimising renewable generation configurations of off-grid green ammonia production systems considering Haber-Bosch flexibility. Energy Convers Manag 2023;280:116790. https://doi.org/10.1016/J.ENCONMAN.2023.116790.

[7] Nayak-Luke R, Bañares-Alcántara R, Wilkinson I. "green" Ammonia: Impact of Renewable Energy Intermittency on Plant Sizing and Levelized Cost of Ammonia. Ind Eng Chem Res 2018;57:14607–16. https://doi.org/10.1021/ACS.IECR.8B02447/ASSET/IMAGES/LARGE/IE-2018-02447Z_0007.JPEG.

[8] Sagel VN, Rouwenhorst KHR, Faria JA. Leveraging Green Ammonia for Resilient and Cost-Competitive Islanded Electricity Generation from Hybrid Solar Photovoltaic–Wind Farms: A Case Study in South Africa. Energy & Fuels 2023. https://doi.org/10.1021/ACS.ENERGYFUELS.3C01950.

[9] Ostuni R, Bialkowski M, Corbetta M. Dynamic Analysis of Casale Green Ammonia Synthesis Process. Boston, MA, USA: 2021.

[10] Mayer P, Ramirez A, Pezzella G, Winter B, Sarathy SM, Gascon J, et al. Blue and green ammonia production: A techno-economic and life cycle assessment perspective. IScience 2023;26:107389. https://doi.org/10.1016/J.ISCI.2023.107389.

[11] Rosa L, Gabrielli P. Energy and food security implications of transitioning synthetic nitrogen fertilizers to net-zero emissions. Environmental Research Letters 2022;18:014008. https://doi.org/10.1088/1748-9326/ACA815.

[12] Salmon N, Bañares-Alcántara R. Impact of grid connectivity on cost and location of green ammonia production: Australia as a case study. Energy Environ Sci 2021;14:6655–71. https://doi.org/10.1039/D1EE02582A.

[13] Campion N, Nami H, Swisher PR, Vang Hendriksen P, Münster M. Techno-economic assessment of green ammonia production with different wind and solar potentials. Renewable and Sustainable Energy Reviews 2023;173. https://doi.org/10.1016/j.rser.2022.113057.

[14] Terlouw T, Bauer C, McKenna R, Mazzotti M. Large-scale hydrogen production via water electrolysis: a techno-economic and environmental assessment. Energy Environ Sci 2022;15:3583–602. https://doi.org/10.1039/d2ee01023b.

[15] Cegla M, Semrau R, Tamagnini F, Engell S. Flexible process operation for electrified chemical plants. Curr Opin Chem Eng 2023;39:100898. https://doi.org/10.1016/J.COCHE.2023.100898.

[16] Frohlke Ulrik. Topsoe signs agreement on first commercial size dynamic green ammonia plant in China. 2023.

[17] Envision - Net Zero Tech Partner. Envision Energy-Green Hydrogen and Green Ammonia Business. 2023.

[18] Alfa-Laval, Hafnia, Haldor-Topsoe, Vestas, Siemens-Gamesa. Ammonfuel-an industrial view of ammonia as a marine fuel. 2020.

[19] The world's first dynamic Green Ammonia Plant | Explore REDDAP n.d. https://stateofgreen.com/en/solutions/reddap-the-worlds-first-dynamic-green-ammonia-plant/ (accessed October 9, 2023).

[20] China: scaling-up "flexible" ammonia production powered by renewable energy – Ammonia Energy Association n.d. https://www.ammoniaenergy.org/articles/china-scaling-up-flexible-ammonia-production-powered-by-renewable-energy/ (accessed October 9, 2023).

[21] Armijo J, Philibert C. Flexible production of green hydrogen and ammonia from variable solar and wind energy: Case study of Chile and Argentina. Int J Hydrogen Energy 2020;45:1541–58. https://doi.org/10.1016/j.ijhydene.2019.11.028.

[22] Rouwenhorst K. Flexible ammonia synthesis: shifting the narrative around hydrogen storage. Ammonia Energy Association 2023. https://www.ammoniaenergy.org/articles/flexible-ammonia-synthesis-shifting-the-narrative-around-hydrogen-storage/ (accessed March 21, 2024).

[23] European Commission. EU's hydrogen strategy 2022. https://energy.ec.europa.eu/topics/energy-systems-integration/hydrogen_en (accessed March 15, 2024).

[24] IEA. Towards hydrogen definitions based on their emissions intensity. 2023.

[25] IEA. Gas Market Report, Q4-2022. 2022.

[26] Gabrielli P, Gazzani M, Martelli E, Mazzotti M. Optimal design of multi-energy systems with seasonal storage. Appl Energy 2018;219:408–24. https://doi.org/10.1016/j.apenergy.2017.07.142.

[27] Dincer I, Rosen MA, Ahmadi P. Optimization of Energy Systems. New York: Wiley; 2017.

[28] Kochenderfer MJ, Wheeler TA. Algorithms for Optimization. Massachusetts: Mit Press; 2019.

[29] Gurobi. gurobipy · PyPI n.d. https://pypi.org/project/gurobipy/ (accessed October 9, 2023).

[30] Gurobi. The Leader in Decision Intelligence Technology - Gurobi Optimization n.d. https://www.gurobi.com/ (accessed October 9, 2023).

[31] Morgan ER. Techno-Economic Feasibility Study of Ammonia Plants Powered by Offshore Wind. University of Massachusetts Amherst, 2013. https://doi.org/10.7275/11kt-3f59.

[32] Sánchez A, Martín M. Scale up and scale down issues of renewable ammonia plants: Towards modular design. Sustain Prod Consum 2018;16:176–92. https://doi.org/10.1016/J.SPC.2018.08.001.

[33] IEA. Ammonia Technology Roadmap - Towards more sustainable nitrogen fertiliser production. 2021.

[34] Pandya HP. Innovative Revamping of Ammonia plants for Capacity up and Energy Efficiency. AmmoniaKnowHow n.d. https://ammoniaknowhow.com/innovative-revamping-ammonia-plants-capacity-energy-efficiency/ (accessed March 15, 2024).

[35] European Commission. Agricultural land prices by region - Data Europa EU 2024. https://data.europa.eu/data/datasets/wctmbzzccaz8tgh9pqqlg?locale=en (accessed March 16, 2024).

[36] Mingolla S, Gabrielli P, Manzotti A, Robson MJ, Rouwenhorst K, Ciucci F, et al. Effects of emissions caps on the costs and feasibility of low-carbon hydrogen in the European ammonia industry. Https://GithubCom/Hkust-Suscity/Electrolytic-Ammonia-Production-in-Europe/Tree/Hydrogen_v100 2024. https://doi.org/10.5281/ZENODO.10771014.

[37] Hydrogen Science Coalition. Clean Hydrogen Definition. 2022.

[38] IRENA. Renewable Power Generation Costs in 2020. 2021.

[39] IRENA. Wind and Solar PV - what we need by 2050. 2020.

[40] Ong S, Campbell C, Denholm P, Margolis R, Heath G. Land-Use Requirements for Solar Power Plants in the United States. 2013.

[41] Denholm P, Hand M, Jackson M, Ong S. Land-Use Requirements of Modern Wind Power Plants in the United States. 2009.

[42] Gagne D. Tribal Options Analysis Rules of Thumb: Solar, Wind, and Biomass. 2019.

[43] Tao M, Azzolini JA, Stechel EB, Ayers KE, Valdez TI. Review—Engineering challenges in green hydrogen production systems. J Electrochem Soc 2022;169:054503. https://doi.org/10.1149/1945-7111/ac6983.

[44] Nugent D, Sovacool BK. Assessing the lifecycle greenhouse gas emissions from solar PV and wind energy: A critical meta-survey. Energy Policy 2014;65:229–44. https://doi.org/10.1016/J.ENPOL.2013.10.048.

[45] Hydrohub Innovation Program. A One-GigaWatt Green-Hydrogen Plant - Advanced Design and Total Installed-Capital Costs. 2022.

[46] Morgan E, Manwell J, McGowan J. Wind-powered ammonia fuel production for remote islands: A case study. Renew Energy 2014;72:51–61. https://doi.org/10.1016/J.RENENE.2014.06.034.

[47] Ikäheimo J, Kiviluoma J, Weiss R, Holttinen H. Power-to-ammonia in future North European 100 % renewable power and heat system. Int J Hydrogen Energy 2018;43:17295–308. https://doi.org/10.1016/J.IJHYDENE.2018.06.121.

[48] Knop V. A World Of Energy - Alkaline electrolyser 2023. https://www.awoe.net/Water-Electrolysis-Alkaline-Part-Load.html (accessed March 21, 2024).

[49] Noch W, Day L, Chang F. Deliverable 1.1 H 2 production and consumption profiles. FCH 2021. https://hypster-project.eu/wp-content/uploads/2021/10/Deliverable_1-1_H2-production_and_consumption_profiles.pdf (accessed March 21, 2024).

[50] Gerloff N. Comparative Life-Cycle-Assessment analysis of three major water electrolysis technologies while applying various energy scenarios for a greener hydrogen production. J Energy Storage 2021;43:102759. https://doi.org/10.1016/J.EST.2021.102759.

[51] Palmer G, Roberts A, Hoadley A, Dargaville R, Honnery D. Life-cycle greenhouse gas emissions and net energy assessment of large-scale hydrogen production via electrolysis and solar PV. Energy Environ Sci 2021;14:5113–31. https://doi.org/10.1039/D1EE01288F.

[52] NREL. Utility-Scale Battery Storage. 2023.

[53] Petkov I, Gabrielli P. Power-to-hydrogen as seasonal energy storage: an uncertainty analysis for optimal design of low-carbon multi-energy systems. Appl Energy 2020;274:115197. https://doi.org/10.1016/J.APENERGY.2020.115197.

[54] Emilsson E, Dahllöf L. Lithium-Ion Vehicle Battery Production Status 2019 on Energy Use, CO2 Emissions, Use of Metals, Products Environmental Footprint, and Recycling. 2019.

[55] Sánchez A, Martín M. Scale up and scale down issues of renewable ammonia plants: Towards modular design. Sustain Prod Consum 2018;16:176–92. https://doi.org/10.1016/J.SPC.2018.08.001.

[56] Bañares-Alcántara R, Dericks III G, Fiaschetti M, Grünewald P, Masa Lopez J, Tsang E, et al. Analysis of Islanded NH3-based Energy Storage Systems Analysis of Islanded Ammonia-based Energy Storage Systems. 2015.

[57] Arnaiz del Pozo C, Cloete S. Techno-economic assessment of blue and green ammonia as energy carriers in a low-carbon future. Energy Convers Manag 2022;255:115312. https://doi.org/10.1016/J.ENCONMAN.2022.115312.

[58] Papadias DD, Peng JK, Ahluwalia RK. Hydrogen carriers: Production, transmission, decomposition, and storage. Int J Hydrogen Energy 2021;46:24169–89. https://doi.org/10.1016/J.IJHYDENE.2021.05.002.

[59] European Commission. Dashboard for Energy Prices in the EU and Main Trading Partners. 2020.

[60] Bastos J, Monforti-Ferrario F, Melica G. GHG Emission Factors for Electricity Consumption. European Commission, Joint Research Centre (JRC). 2024.

[61] Copernicus Climate Change Service. Climate and energy indicators for Europe from 1979 to present derived from reanalysis. 2020. https://doi.org/10.24381/cds.4bd77450.

[62] Csutar VG, Kallikuppa S, Charles L. Introduction to HVDC Architecture and Solutions for Control and Protection. 2021.

[63] Specht M. Renewable Energy Curtailment 101: The Problem That's Actually Not a Problem At All 2019. https://blog.ucsusa.org/mark-specht/renewable-energy-curtailment-101/ (accessed August 29, 2023).

[64] Cevik S, Ninomiya K. Chasing the Sun and Catching the Wind: Energy Transition and Electricity Prices in Europe. 2022.

[65] European Commission. Effect of high shares of renewables on power systems. Publications Office of the European Union; 2019. https://doi.org/10.2833/021194.

[66] Tselika K. The impact of variable renewables on the distribution of hourly electricity prices and their variability: A panel approach. Energy Econ 2022;113:106194. https://doi.org/10.1016/J.ENECO.2022.106194.

[67] Augustine C, Blair N. Storage Futures Study: Storage Technology Modeling Input Data Report 2021. https://doi.org/10.2172/1785959.

[68] Ramasamy V, Zuboy J, O'Shaughnessy E, Feldman D, Desai J, Woodhouse M, et al. U.S. Solar Photovoltaic System and Energy Storage Cost Benchmarks, With Minimum Sustainable Price Analysis: Q1 2022 2022. https://doi.org/10.2172/1891204.

[69] Kebede AA, Kalogiannis T, Van Mierlo J, Berecibar M. A comprehensive review of stationary energy storage devices for large scale renewable energy sources grid integration. Renewable and Sustainable Energy Reviews 2022;159:112213. https://doi.org/10.1016/J.RSER.2022.112213.

[70] Cole W, Frazier AW, Augustine C. Cost Projections for Utility-Scale Battery Storage: 2021 Update. 2021.

[71] David WIF, Agnew GD, Bañares-Alcántara R, Barth J, Bøgild Hansen J, Bréquigny P, et al. 2023 roadmap on ammonia as a carbon-free fuel. JPhys Energy 2024;6. https://doi.org/10.1088/2515-7655/ad0a3a.

[72] Schmidt O, Gambhir A, Staffell I, Hawkes A, Nelson J, Few S. Future cost and performance of water electrolysis: An expert elicitation study. Int J Hydrogen Energy 2017;42:30470–92. https://doi.org/10.1016/J.IJHYDENE.2017.10.045.

[73] Risco-Bravo A, Varela C, Bartels J, Zondervan E. From green hydrogen to electricity: A review on recent advances, challenges, and opportunities on power-to-hydrogen-to-power systems. Renewable and Sustainable Energy Reviews 2024;189:113930. https://doi.org/10.1016/J.RSER.2023.113930.

[74] IRENA. Green Hydrogen Cost Reduction: Scaling Up Electrolysers To Meet The 1.5°C Climate Goal. 2020.

[75] Cheng M, Verma P, Yang Z, Axelbaum RL. Flexible cryogenic air separation unit—An application for low-carbon fossil-fuel plants. Sep Purif Technol 2022;302:122086. https://doi.org/10.1016/J.SEPPUR.2022.122086.

[76] Topsoe | Efficient green ammonia plants for power-to-X projects n.d. https://www.topsoe.com/processes/green-ammonia (accessed February 20, 2024).

[77] European Hydrogen Bank - European Commission n.d. https://energy.ec.europa.eu/topics/energy-systems-integration/hydrogen/european-hydrogen-bank_en (accessed March 22, 2024).

[78] Oni AO, Anaya K, Giwa T, Di Lullo G, Kumar A. 45V or 45Q? How Tax Credits Will Influence Low-Carbon Hydrogen's Development. Energy Convers Manag 2024;254. https://doi.org/10.1016/j.enconman.2022.115245.

[79] Cesaro Z, Ives M, Nayak-Luke R, Mason M, Bañares-Alcántara R. Ammonia to Power: Forecasting the Levelized Cost of Electricity from Green Ammonia in Large-scale Power Plants. Appl Energy 2021;282.

[80] Hydrohub Innovation Program. Safety Aspects of Green Hydrogen Production on Industrial Scale Acknowledgements. 2023.

[81] Eljechtimi A. Morocco's OCP Plans $7 Billion Green Ammonia Plant to Avert Supply Problems. 2023.

[82] Ammpower. Movement Toward Small-scale Ammonia Production in 2023 2022. https://www.iamm.green/ammonia-production-accelerating/ (accessed March 22, 2024).

Supplementary Information

Investment cost:

$$I_k^{NPV} = \sum_{l=0}^{L} \frac{I_{k,l}}{(1+r)^l} \qquad \textit{SI - eq. i}$$

Where I_k^{NPV} represents the net present value of the installation cost of technology k and r is the discount rate. I_k is equal to the cost of the technology multiplied by the installed capacity *SI - eq. ii*.

$$I_k = c_k \dot{P}_k \qquad \textit{SI - eq. ii}$$

Similarly, $v_k^{NPV} I_k$ is the net present value of operation and maintenance cost (O&M). O&M are presented as a fraction of the installation cost.

$$v_k^{NPV} = \sum_{l=1}^{L} \frac{I_{k,l}}{(1+r)^l} \qquad \textit{SI - eq. iii}$$

Renewable installations:

The hourly power generation, $V_{E,k_R,t}$ from PV and WT results from *SI - eq. iv*.

$$V_{E,k_R,t} = \eta_{k_R} \omega_{R,t} \dot{P}_{k_R}, \forall\, k \in K_R \qquad \textit{SI - eq. iv}$$

where $\mathcal{K}_R$ is the set of renewable energy technologies $\{PV, WT\}$; η_{k_R} is the transmission efficiency of solar PV and WT; $\omega_{R,t}$ is the time-dependent capacity factor of solar and wind energy and $\dot{P}_{k_R}$ is the installed capacity of PV and WT.

$$b_k \dot{P}_{k,min} \leq \dot{P}_k \leq b_k \dot{P}_{k,max}, \forall\, k \in \mathcal{K}_R \qquad \textit{SI - eq. v}$$

We set a maximum installation size according to *SI - eq. v*, where b_k is a binary variable indicating whether the technology is installed or not.

Imported electricity from the grid:

The amount of energy that can be imported to the plant from the grid is constrained by the hourly electricity demand of the main subsystems of the plant, namely the electrolyzers, air separation unit (ASU), and ammonia synthesis loop (*SI - eq. vi*). Similarly, since the High-Voltage Alternating Current (HVAC) transmission lines connecting the plant to the grid are built based on this maximum capacity, the amount of electricity that can be sold back to the grid is also constrained to this amount per hour.

$$0 \leq M_{E,t} \leq U_{E,EL,t} + U_{E,A,t} + U_{E,S,t}, \forall\, t \in \{0, \ldots, T\} \qquad \textit{SI - eq. vi}$$

Li-ion batteries:

The quantity of renewable electricity stored in BESS during hour t $S_{E,B,t}$ is calculated by subtracting the loss of electricity resulting from the self-discharge of the batteries, $\lambda_B \Delta_t$ from the energy stored in the previous hour, $S_{E,B,t-1}$, by adding the electricity entering the battery during hour t $U_{E,B,t}$ multiplied

by the charging efficiency of the battery η_B^c and subtracting the electricity output from the battery during the same hour, $V_{E,B,t}$ divided by the discharging efficiency η_B^d, according to *SI - eq. vii*.

$$S_{E,B,t} = (1 - \lambda_B \Delta_t) S_{E,B,t-1} + \eta_B^c U_{E,B,t} - \frac{V_{E,B,t}}{\eta_B^d}, \forall\, t \in \{1, ..., T\} \qquad \textit{SI - eq. vii}$$

The amount of electricity entering the BESS and the hourly maximum output of the BESS are constrained by the minimum number of time intervals for full charge, τ^c and discharge, τ^d (*SI - eq. viii* and *SI - eq. ix*) while the quantity stored at time t is constrained by the maximum installed capacity $\dot{P}_B$ (*SI - eq. x*).

$$0 \leq U_{E,B,t} \leq \frac{\dot{P}_B}{\tau^c}, \forall\, t \in \{0, ..., T\} \qquad \textit{SI - eq. viii}$$

$$0 \leq V_{E,B,t} \leq \frac{\dot{P}_B}{\tau^d}, \forall\, t \in \{0, ..., T\} \qquad \textit{SI - eq. ix}$$

$$0 \leq S_{E,B,t} \leq b_B \dot{P}_B, \forall\, t \in \{0, ..., T\} \qquad \textit{SI - eq. x}$$

Lastly, we include periodicity constraints (*SI - eq. xi*) to ensure the reproducibility and sustainability of the optimal operation strategy beyond the considered time horizon.

$$S_{E,B,T-1} = S_{E,B,0} \qquad \textit{SI - eq. xi}$$

Electrolyzers:

The minimum installed capacity of the electrolyzer, denoted as $\dot{P}_{EL,min}$ is set to ensure that the system can produce sufficient hydrogen to meet the minimum hourly demand, considering 24-hour continuous production. In other words, if the installed capacity is less than $\dot{P}_{EL,min}$, the system will not be able to produce enough hydrogen to satisfy the minimum production constraint, even when operating at full capacity throughout the day (*SI - eq. xii*).

$$\dot{P}_{EL,min} \leq \dot{P}_{EL} \leq \dot{P}_{EL,max} \qquad \textit{SI - eq. xii}$$

$\dot{P}_{EL,min}$ results from *SI - eq. xiii* where ρ represent the stoichiometric ratio hydrogen/ammonia by mass and $\eta_{H2,E,EL}$ the electrolyzer conversion efficiency.

$$\dot{P}_{EL,min} = \rho\, D_{NH3}^h\, \eta_{H2,E,EL} \qquad \textit{SI - eq. xiii}$$

The model optimizes the hourly hydrogen output of the electrolyzer, $V_{H2,EL,t}$ by considering the conversion efficiency of the electrolyzer, $\eta_{E,H2,EL}$, which is multiplied by the input electricity during the corresponding hour, $U_{E,EL,t}$, according to *SI - eq. xiv*.

$$V_{H2,EL,t} = \eta_{E,H2,EL} U_{E,EL,t}, \forall\, t \in \{0, ..., T\} \qquad \textit{SI - eq. xiv}$$

Lastly, we set the minimum load of the electrolyzer δ_{EL} to 10% of the nominal capacity *SI - eq. xv*.

$$\delta_{EL} \dot{P}_{EL} \leq U_{E,EL,t} \leq \dot{P}_{EL}, \forall\, t \in \{0, ..., T\} \qquad \textit{SI - eq. xv}$$

Hydrogen compressors and high-pressure storage tanks:

The model optimizes the hourly input electricity, $U_{E,CP,t}$ and output hydrogen of the compressor, $V_{H2,CP,t}$ as follow (*SI - eq. xvi*):

$$V_{H2,CP,t} = \eta_{E,H2,CP}\, U_{E,CP,t}, \forall\, t \in \{0, ..., T\}$$ *SI - eq. xvi*

Where the conversion efficiency of the electrolyzer is $\eta_{E,H2,CP}$. Notably, we assume no hydrogen losses during the compressor phase (*SI - eq. xvii*).

$$U_{H2,CP,t} = V_{H2,CP,t}, \forall\, t \in \{0, ..., T\}$$ *SI - eq. xvii*

Once compressed, the output hydrogen of the compressor, $V_{H2,CP,t}$, directly becomes the input hydrogen of the storage tanks $U_{H2,ST,t}$.

$$U_{H2,ST,t} = V_{H2,CP,t}, \forall\, t \in \{1, ..., T\}$$ *SI - eq. xviii*

At each time step t, the amount of stored hydrogen, $S_{H2,ST,t}$ is determined by adding the previously stored hydrogen, $S_{H2,ST,t-1}$, to the incoming hydrogen from the compressor, $U_{H2,ST,t}$, and subtracting the hydrogen that exits the storage tanks, $V_{H2,ST,t}$ for use in the ammonia synloop (SI - eq. xix*)*. No self-discharge losses are considered for hydrogen storage.

$$S_{H2,ST,t} = S_{H2,ST,t-1} + U_{H2,ST,t} - V_{H2,ST,t}, \forall\, t \in \{1, ..., T\}$$ *SI - eq. xix*

Air separator unit (ASU):

We choose a minimum load, δ_A of 50% for the semi-flexible plant and 10% for the fully-flexible plant. Hence, the hourly electricity input of the ASU, $U_{E,A,t}$ is constrained according to *SI - eq. xx*.

$$\delta_A \dot{P}_A \leq U_{E,A,t} \leq \dot{P}_A, \forall\, t \in \{0, ..., T\}$$ *SI - eq. xx*

The nitrogen output, $V_{N2,A,t}$ is equal to the conversion efficiency of the ASU, $\eta_{E,N2,A}$ multiplied by the electricity input (*SI - eq. xxi*).

$$V_{N2,A,t} = \eta_{E,N2,A}\, U_{E,A,t}, \forall\, t \in \{0, ..., T\}$$ *SI - eq. xxi*

Similar to the electrolyzer, we set a minimum installed capacity, $\dot{P}_{A,min}$ according to *SI - eq. xxii*.

$$\dot{P}_{A,min} \leq \dot{P}_A \leq \dot{P}_{A,max}$$ *SI - eq. xxii*

The minimum installed capacity of the ASU, denoted as $\dot{P}_{A,min}$, is set to ensure that the system can produce sufficient nitrogen to meet the hourly demand of the ammonia synthesis loop. $\dot{P}_{A,min}$ is computed though *SI - eq. xxiii*.

$$\dot{P}_{A,min} = (1 - \rho)\, D^{h}_{NH3}\, \eta_{N2,E,A}$$ *SI - eq. xxiii*

Ammonia synloop:

As assumed for the ASU, we choose a minimum load, δ_S of 50% for the semi-flexible plant and 10% for the fully flexible plant (***Error! Reference source not found.***.

$$\delta_S \dot{P}_S \leq U_{E,S,t} \leq \dot{P}_S, \forall\, t \in \{0, ..., T\}$$ *SI - eq. xxiv*

The ammonia output, $V_{NH3,S,t}$ is equal to the conversion efficiency of the ammonia synloop, $\eta_{E,NH3,S}$ multiplied by the electricity input (*SI - eq. xxv*).

$$V_{NH3,S,t} = \eta_{E,NH3,S}\, U_{E,S,t}, \forall\, t \in \{0, ..., T\}$$ *SI - eq. xxv*

The minimum installed capacity, $\dot{P}_{S,min}$ is computed as for the ASU (*SI - eq. xxvi*).

$$\dot{P}_{S,min} = \left(D^{h}_{NH3}\right)\eta_{NH3,E,S} \qquad \textit{SI - eq. xxvi}$$

The hourly hydrogen, $U_{H2,S,t}$ and nitrogen inputs, $U_{N2,S,t}$ are regulated by *SI - eq. xxvii* and *xxviii*, respectively.

$$U_{H2,S,t} = \rho(V_{NH3,S,t}), \forall\, t \in \{0, ..., T\} \qquad \textit{SI - eq. xxvii}$$

$$U_{N2,S,t} = (1 - \rho)V_{NH3,S,t}, \forall\, t \in \{0, ..., T\} \qquad \textit{SI - eq. xxviii}$$

As for ASUs2.2.7, in a continuous plant installed capacity of the ammonia synloop $\dot{P}_S$ equals the minimum capacity, $\dot{P}_{S,min}$, and a continuous operation is assumed.

Cryogenic storage:

The amount of stored ammonia at time t, $S_{NH3,CT,t}$, is regulated by *SI - eq. xxix*, where $U_{NH3,CT,t}$ is the volume of ammonia entering the storage tank while $V_{NH3,CT,t}$ is the output ammonia. $U_{NH3,CT,t}$ is set to be smaller or equal than the ammonia output of the synloop $V_{NH3,S,t}$ to not incur in energy imbalances (*SI - eq. xxx*). Notably, we do not assume any loss of ammonia during cryogenic storage.

$$S_{NH3,CT,t} = S_{NH3,CT,t-1} + U_{NH3,CT,t} - V_{NH3,CT,t},\ \forall\, t \in \{1, ..., T\} \qquad \textit{SI - eq. xxix}$$

$$U_{NH3,CT,t} \leq V_{NH3,S,t},\ \forall\, t \in \{0, ..., T\} \qquad \textit{SI - eq. xxx}$$

Text 1:

Previous studies, including Nugent & Sovacool[1], have conducted extensive literature reviews, and found that PV emits more carbon per MWh compared to wind turbines, specifically 49.91 kg CO_2/MWh for PV and 34.11 kg CO_2/MWh for wind turbines. However, there is notable uncertainty within this range. To calculate the average electricity produced in MWh per year by a 1 MW wind turbine or solar installation, we multiply 8760 hours by the average worldwide capacity factor for wind (23%[2]) and solar (12%[3]). This approach enables the determination of lifecycle emissions from a MW of installed solar and wind capacity.

Lifecycle emissions data for key components of the hydrogen production and storage system were collected from various sources. For lithium-ion batteries, data were taken from Emilsson and Dahllöf[4]. Emissions data for electrolyzers were sourced from[5,6], while data for hydrogen compressors and storage tanks were obtained from Palmer et al.[5]. Other ancillary components, such as piping, valves, and control systems, were not included in our lifecycle emissions analysis, as their carbon content is considered minimal compared to the key subsystems mentioned above.

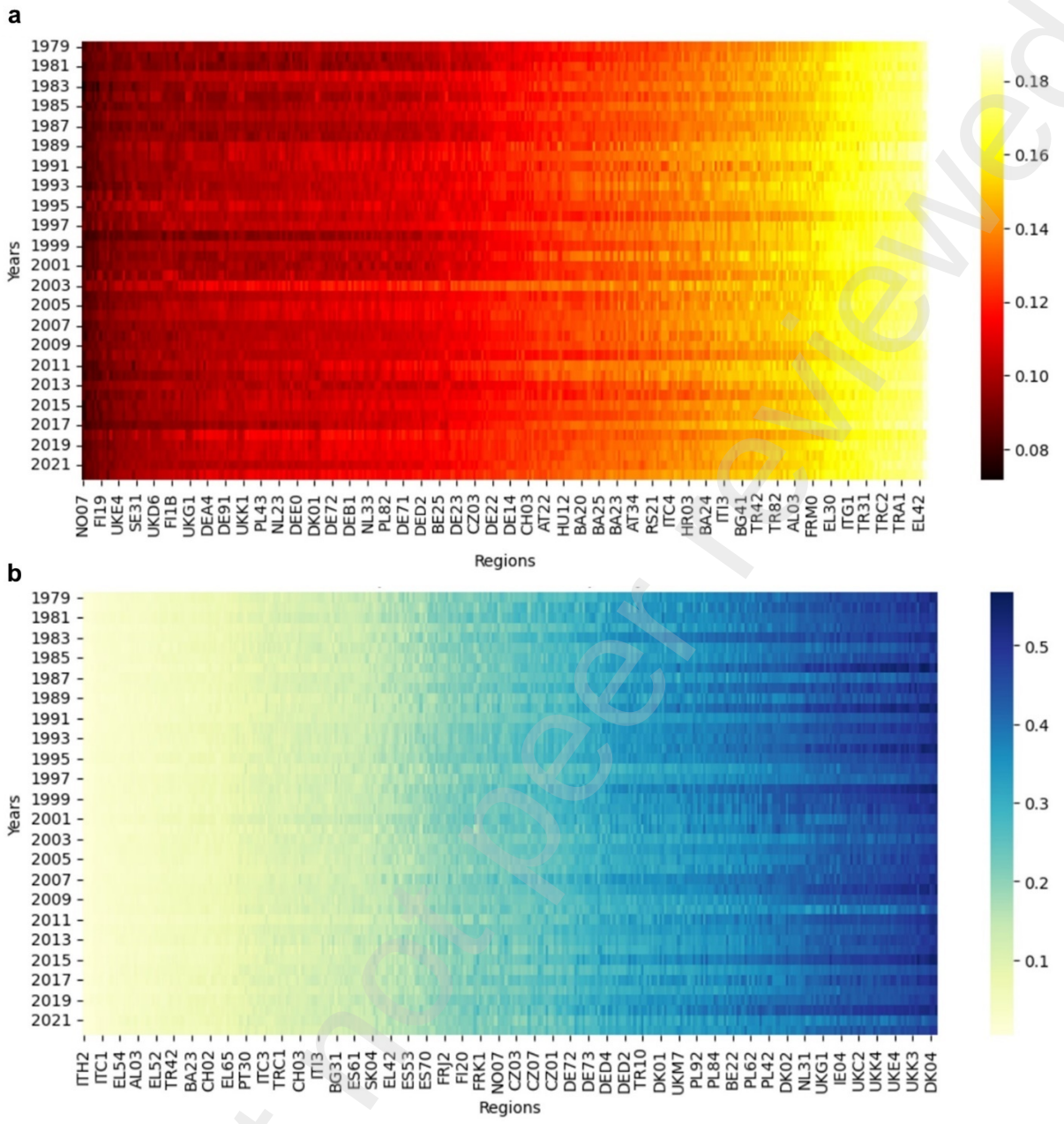

SI - Fig. i: **Historical (1979-2022) solar and wind average capacity factors for NUTS-2 European regions.** Capacity factors based on the Copernicus Climate Change Service (C3S) dataset [7]. **a** illustrates the average annual solar capacity factors, while **b** shows the average annual wind capacity factors.

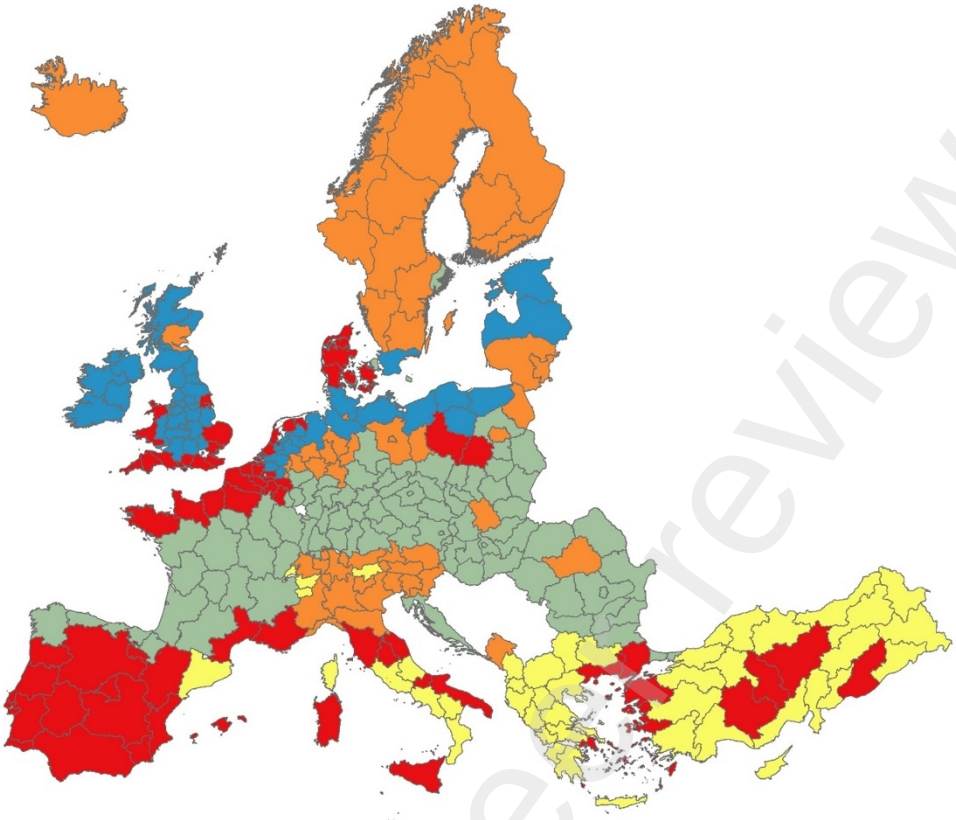

		Mean annual solar CF			
		75th-100th	50th-74th	25th-49th	0th-24th
Mean annual wind CF	75th-100th	High-capacity	High-capacity	High-capacity	Wind-dominated
	50th-74th	High-capacity	Median-capacity	Median-capacity	Low-capacity
	25th-49th	High-capacity	Median-capacity	Median-capacity	Low-capacity
	0th-24th	Solar-dominated	Low-capacity	Low-capacity	Low-capacity

SI - Fig. ii: European regions clustered based on their capacity factor of solar and wind energy. The color code indicates the cluster to which each region belongs: High-capacity regions (red), Median-capacity regions (green), Low-capacity regions (orange), Solar-dominated regions (yellow), and Wind-dominated regions (blue).

SI - Table i: Levelized Cost of Ammonia (LCOA) comparison for semi-islanded and islanded (off-grid) ammonia plants across five representative regions and three plant configurations. The semi-islanded plants can import grid electricity as long as they do not violate the 1 kg CO_2e/kg H_2 emission constraint, while the off-grid plants have a strict 0 kg CO_2e/kg H_2 emission constraint. The "Difference" column represents the percentage cost increase for the off-grid scenario compared to the semi-islanded scenario.

Region	Continuous			Semi-flexible			Fully-flexible		
	1 kg CO_2e/kg H_2	0 kg CO_2e/kg H_2	Difference	1 kg CO_2e/kg H_2	0 kg CO_2e/kg H_2	Difference	1 kg CO_2e/kg H_2	0 kg CO_2e/kg H_2	Difference
Median-capacity	1374.7	1845.0	34%	1334.9	2742.4	105%	1334.9	1483.6	11%
High-capacity	1057.6	2145.6	103%	1001.5	1706.4	70%	965.5	1084.2	12%
Low-capacity	2311.4	7249.0	214%	2325.3	4597.7	98%	2223.5	2619.0	18%
Solar-dominated	1433.5	2402.9	68%	1527.3	1848.3	21%	1415.1	1545.4	9%
Wind-dominated	869.8	1534.0	76%	813.5	2892.8	256%	761.9	1104.9	45%

Supplementary Bibliography

[1] Nugent D, Sovacool BK. Assessing the lifecycle greenhouse gas emissions from solar PV and wind energy: A critical meta-survey. Energy Policy 2014;65:229–44. https://doi.org/10.1016/J.ENPOL.2013.10.048.

[2] ENERGYDATA. Global Wind Atlas 2023. https://globalwindatlas.info/en (accessed September 2, 2023).

[3] ENERGYDATA. Global Solar Atlas 2023. https://www.globalsolaratlas.info/map?c=-5.103367,-29.003906,2&s=27.081337,8.789063&m=site (accessed September 2, 2023).

[4] Emilsson E, Dahllöf L. Lithium-Ion Vehicle Battery Production Status 2019 on Energy Use, CO2 Emissions, Use of Metals, Products Environmental Footprint, and Recycling. 2019.

[5] Palmer G, Roberts A, Hoadley A, Dargaville R, Honnery D. Life-cycle greenhouse gas emissions and net energy assessment of large-scale hydrogen production via electrolysis and solar PV. Energy Environ Sci 2021;14:5113–31. https://doi.org/10.1039/D1EE01288F.

[6] Gerloff N. Comparative Life-Cycle-Assessment analysis of three major water electrolysis technologies while applying various energy scenarios for a greener hydrogen production. J Energy Storage 2021;43:102759. https://doi.org/10.1016/J.EST.2021.102759.

[7] Copernicus Climate Change Service. Climate and energy indicators for Europe from 1979 to present derived from reanalysis. 2020. https://doi.org/10.24381/cds.4bd77450.